Experimental validation of hygrothermal models for building materials and walls: an analysis of recent trends

Thomas Busser, Julien Berger, Amandine Piot, Mickael Pailha, Monika Woloszyn

Thomas Busser
Univ. Grenoble Alpes, Univ. Savoie Mont Blanc, CNRS, LOCIE, 73000 Chambéry, France
University Grenoble Alpes, CEA, LITEN, DTS, INES, F-38000, Grenoble, France

Julien Berger
Univ. Grenoble Alpes, Univ. Savoie Mont Blanc, CNRS, LOCIE, 73000 Chambéry, France

Amandine Piot
University Grenoble Alpes, CEA, LITEN, DTS, INES, F-38000, Grenoble, France

Mickael Pailha
Univ. Grenoble Alpes, Univ. Savoie Mont Blanc, CNRS, LOCIE, 73000 Chambéry, France

Monika Woloszyn
Univ. Grenoble Alpes, Univ. Savoie Mont Blanc, CNRS, LOCIE, 73000 Chambéry, France

Experimental validation of hygrothermal models for building materials and walls: an analysis of recent trends

Experimental validation of hygrothermal models for building materials and walls: an analysis of recent trends

Thomas Busser[1,2], Julien Berger[1], Amandine Piot[2], Mickael Pailha[1], Monika Woloszyn[1]

Abstract

Models for the prediction of heat and mass transfers in building porous material have been developed since the 90's with simulation programs such as MATCH, UMIDUS, DELPHIN and Wufi. These models are used to analyse the physical phenomena occurring and particularly the impact of moisture on buildings' energy performance and durability. With this goal in mind, it is important to validate the representation of the physical phenomena made by the numerical models. This article reviews recent studies comparing the results obtained with numerical models and experimental data. An overall trend can be observed for most of these studies, highlighting that the experimental front always rushes faster than the simulation results. Therefore, this study analyses theses comparison to explain these discrepancies based on the effects of (i) the type of materials, (ii) the boundary conditions, (iii) the scale of the design facility, (iv) the model used to describe the physical phenomena and (v) the influence of the model input parameter. The general trend shows that discrepancies are observed most particularly for highly hygroscopic or bio-based materials. These discrepancies are also greater for time dynamic boundary conditions, particularly at the scale of the wall. Moreover, some of the assumptions on the properties of the materials used as input in the models are questioned. Indeed, the models considering the hysteresis effects and temperature dependency of the moisture storage capacity show better agreement with experimental data. Finally, the physical phenomena used in the models only consider diffusive transport while it appears that the advective of moisture through the porous material may play an important role.

Keywords

hygrothermal, hygroscopic material, physical phenomena, comparison, discrepancies

[1] LOCIE, University Savoie Mont Blanc - CNRS, F-73000, Chambéry, France
[2] University Grenoble Alpes, CEA, LITEN, DTS, INES, F-38000, Grenoble, France

Contents

1 Introduction

Indoor air relative humidity can affect energy consumption and building performance [1, 2, 3, 4], durability of materials [5], perceived indoor air quality and indoor climate of buildings [6, 7, 8]. Therefore, hygroscopic materials are increasingly used to control the indoor moisture level by absorbing and releasing moisture [9, 10, 11, 12]. This moisture buffering is quantified by the moisture buffering value (MBV) of materials, which is influenced by several parameters such as moisture load (initial and boundary conditions) [11], ventilation rate [13] and material properties [14, 15, 16, 17].

The key is to understand the physical processes influencing heat and moisture transport within hygroscopic materials and to model them. Numerical simulation tools are used to analyse these physical phenomena and make predictions. During the past few decades, many hygrothermal simulation tools have been developed [18, 19] with this aim in mind. Before to predict the hygrothermal behaviour, it is necessary to validate the modelling of physical phenomena with experimental measurements.

Several studies have been reported in the literature where experimental results for different materials are compared to simulation results. In general, these unsteady-state data include both adsorption and desorption phase, as shown in 1. A material, with an initial moisture content w_0, is submitted to an adsorption phase at relative humidity ϕ_1 and then to a desorption phase at relative humidity ϕ_2. Discrepancies seem to appear when comparing the results from numerical models and experimental data [20, 21], as illustrated in Figure 1. As we will try to demonstrate further in this paper, the results of the simulation under-estimate both the adsorption and desorption processes. In other words, the experimental moisture front moves faster than the simulation results, as indicated by the discrepancies 1 in Figure 1. Moreover, the steady-state value of the moisture content differs most of the time for both experimental and numerical results, as illustrated by the discrepancies 2. Numerous studies report similar observations and the origin of these deviations is difficult to grasp. The prediction of heat transfer presents fewer problems than moisture transfer, given that the observed deviations remain within the sensors' uncertainty for most cases.

This paper analyses the reported comparisons between the measurement and simulation of hygrothermal behaviour The influence of several parameters will be discussed: (i) the experimental parameters: the desing of the protocol, the type of materials, configuration and the scale of the study; (ii) the boundary conditions and (iii) the modelling of physical phenomena: the description and formulation, the numerical resolution and the influence of material properties. The present article therefore reports the latest studies which compare measurement and simulation results on the hygrothermal behaviour of building materials and investigates potentially emerging trends for all building materials concerning the validation of the simulation tools.

In the first part, the general method used in this article to compare measurement and simulation is described. Then generalities on hygrothermal modelling are reported, together with the description of the transport phenomena. In the major section of the paper, studies comparing experimental results and simulations of hygrothermal behaviour are reviewed. Modelling of the coupled transfers in the different cases is also studied. To improve the prediction of material behaviour, the results are then analysed according to several inputs (material, scale of study, boundary conditions, physical phenomena and material properties).

2 Approach for comparing experiment and simulation

2.1 General approach

The general approach to comparing experimental data to numerical results is illustrated in Figure 2. Two processes can be distinguished. The first one concerns the experiments and the generation of measured data. This required that a sample be submitted to measured boundary conditions according to a previously defined design. Among other tests, the design includes calibration of the sensors, verification of the repeatability of the experiments and computation of the uncertainty measurements. A field representing the physical phenomena occurring in the samples is observed. The observation

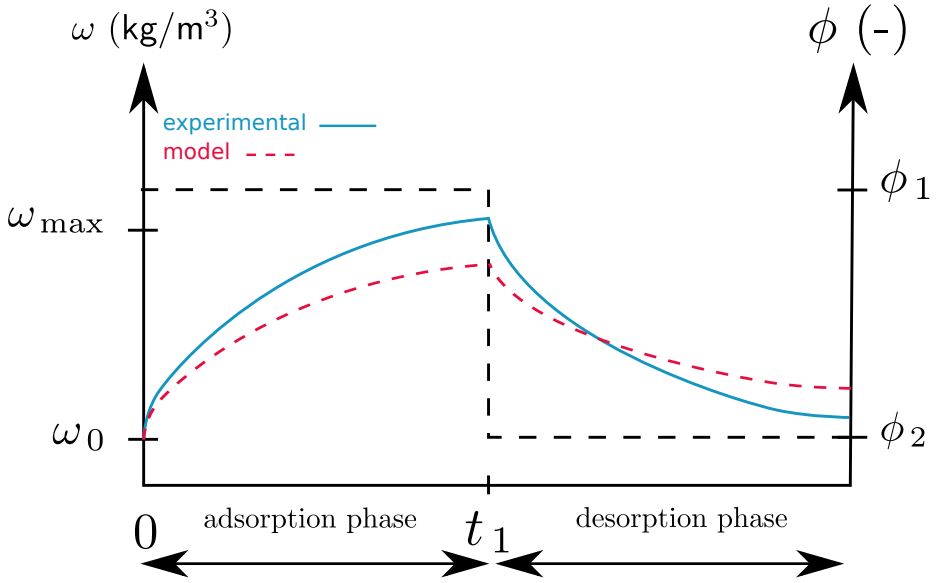

Figure 1: Illustration of the discrepancies when comparing experimental data and numerical results.

can be local at a particular point in the sample as is the case when measuring temperature or relative humidity. An intrusive sensor is necessary in this case. It can also be global when the field is evaluated for the whole scale of the sample, as when measuring the sample mass. In the end, experimental data varying in time are produced. The second process consists in generating numerical results. This requires that a model be built including a mathematical formulation of the physical phenomena associated with a numerical method. The inputs of the model are the measured boundary conditions of the experiments and the material properties. The latter come from a previous step aiming at characterising the material. Several standards are used to generate analytical functions fitting with the measurements of materials characterisation. The results of the model are both local and global are time-dependent.

The experimental data and the numerical results are compared based on the global tendencies as well as the residual between the two fields. Some uncertainties and biases, called b_i in Figure 2, cannot be avoided and impact different elements of the study. Therefore, this comparison must be analysed under these uncertainties and possible biases introduced in the whole process. Four different biases have been identified and are illustrated in Figure 2. The literature review will be discussed in Section 4 according to these possible biases.

The first biases, noted b_1 in Figure 2, are introduced when conducting the experiments and generating the data. There are biases due to uncertainty and noise in measurement, which can be evaluated by computing the propagation of uncertainties. The type of material under investigation, its geometry and in a more general way the configuration of the design including the scale of study may also affect the results. The repeatability, the protocol validation, the sensor calibration, the limitation of side effects, summarised by the protocol in Figure 2, are important aspects of the design that have to be controlled to minimise the biases when comparing the data to numerical results.

Some biases, noted b_2, concern the boundary conditions imposed during the experiment. Sensors are used to measure the boundary conditions with a measurement uncertainty. Moreover, biases may be introduced when neglecting and not measuring certain physical phenomena accurately, such as radiation or convection at the surface of the materials. The solicitations applied to the samples can be time-constant or time-variable. We will see to what extent the type of boundary conditions influence the prediction of results using simulation tools.

Then the model itself introduces biases, noted b_3. The accuracy of the numerical results strongly depends on the physical phenomena included in the model definition. The biases might also come from

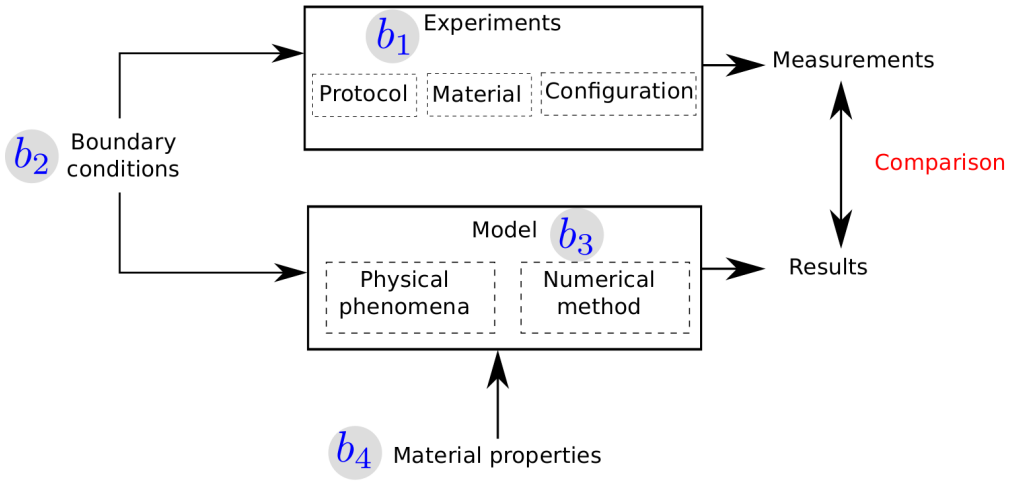

Figure 2: Approach for comparing experimental data and numerical results.

the resolution of the partial differential equations, which can introduce numerical errors. However, this bias should be minimised compared to the hypothesis made on the physical phenomena.

To perform simulations, boundary conditions together with the material properties must be added to the model. These inputs may introduce significant biases in the numerical results obtained. As for the experimental part, the boundary conditions are measured with uncertainties and hypotheses on the physical phenomena that have to be taken into account in the computation of the results. Moreover, the material properties used in the simulation play an important role and are another source of biases, noted b_4. Some materials are extremely heterogeneous and there might be differences between the material characterised and the one used for the design. In addition, the material properties are extrapolated from measurement with their own uncertainties. These measurements should be taken if possible using the same sample as for the experiments: steady-state methods are commonly used (the cup method and the gravimetry).

2.2 Selection of studies

The studies presented below were chosen according to several criteria. We were interested in studies on coupled heat and mass transfers within porous media. The studies had to be applied to building physics, to understand the hygrothermal behaviour of porous materials including both experimental and numerical results. The authors had to detail the experimental facility, protocol and the configuration studied. Moreover, details on the numerical study had to be available, such as the software chosen and the model's assumptions. The measurement and simulation could be compared at different scales: materials, walls or envelope and building. In this paper, we limit the scope to the prediction of transfer within the material or simple wall assemblies to focus on modelling coupled transfer and to avoid other sources of uncertainty.

In the main part of this article, the comparison of results between measurement and simulation is first based on the conclusions of articles summarised. If necessary, an additional analysis of the results was carried out to detail and better quantify the comparison.

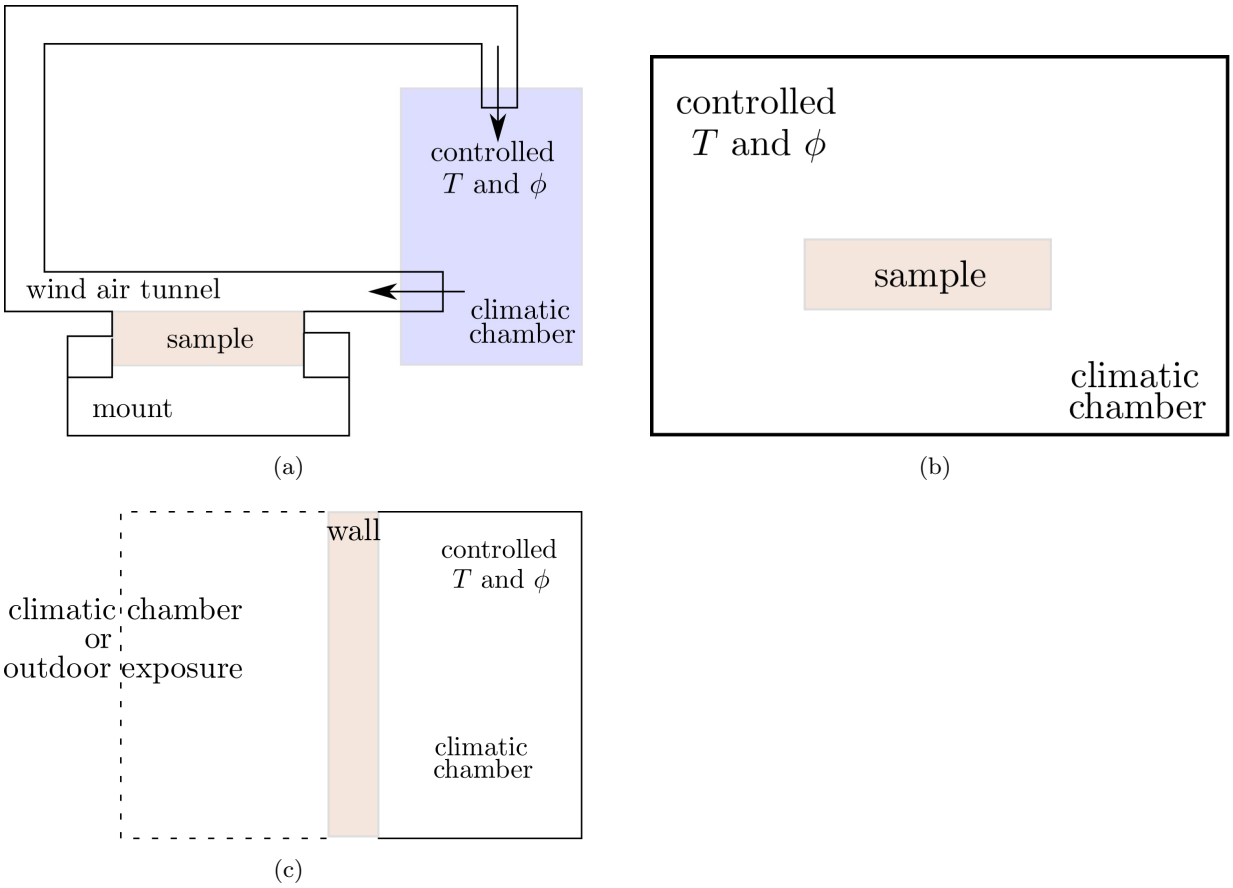

Figure 3: Experimental facility used to investigate the heat and moisture transfers: wind air tunnel (a), climatic chamber (b) and wall scale (c).

2.3 Experimental facilities

Several types of experimental devices were used in the studies reported. The material and wall scales can be considered separately. At the material scale, two types of experimental facilities were distinguished: the climatic chamber and the wind air tunnel. These facilities differ only in the way convective boundary conditions were controlled, nevertheless, both can be used to study the hygrothermal behaviour of a single material exposed to controlled conditions.

In the wind air tunnel (see Figure 3(a)), the top surface of the sample is exposed to an established air flow. The airflow temperature (T) and relative humidity (ϕ) are controlled using an environmental chamber from which the air is delivered. Air speed is also controlled.

In the climatic chamber (Figure 3(b)), the temperature and relative humidity of ambient air are controlled. Saline solutions or a dew point water tank in the chamber can be used for relative humidity and a heat exchanger inside the chamber for temperature. The sample can be exposed either to one relative humidity level or to a gradient of relative humidity: one climatic chamber at each side is needed.

To study the behaviour of walls, samples can be exposed to controlled conditions in climatic chambers or to outdoor conditions at one side and controlled at the other side as illustrated in Figure 3(c). In the first case two climatic chambers are needed, one to simulate indoor conditions and the other for outdoor conditions, both conditions being stationary or time-variable.

2.4 Physical model and mathematical formulation

The models used in the literature for the comparison with experimental data are based on the assumptions that building materials are porous media, containing air and water, in vapour and liquid forms.

In most of the models, air flow is not modelled. The description of physical phenomena is based on the principle of mass and energy conservation and the problem can be formulated as follows:

$$\frac{\partial w}{\partial t} = -\boldsymbol{\nabla}\cdot(\boldsymbol{g}_{\mathrm{v}} + \boldsymbol{g}_{\ell}), \tag{1a}$$

$$\frac{\partial E}{\partial t} = -\boldsymbol{\nabla}\cdot(\boldsymbol{q}_{\mathrm{c}} + \boldsymbol{q}_{\ell\mathrm{v}}). \tag{1b}$$

where w is the moisture content and E the energy.

The moisture transfer occurs due to capillary migration, $\boldsymbol{g}_{\ell}$, and vapour diffusion, $\boldsymbol{g}_{\mathrm{v}}$. The vapour diffusion can be driven by the vapour pressure gradient and the temperature gradient (called thermal diffusion):

$$\boldsymbol{g}_{\mathrm{v}} = -\delta_{\mathrm{v}}\boldsymbol{\nabla}P_{\mathrm{v}} - \delta_{\mathrm{T}}\boldsymbol{\nabla}T, \tag{2a}$$

$$\boldsymbol{g}_{\ell} = -\delta_{\ell}\boldsymbol{\nabla}P_{\mathrm{c}}. \tag{2b}$$

where δ_{v} stands for the vapour permeability, δ_{T} the permeability for temperature-driven vapour diffusion and δ_{ℓ} denotes the liquid permeability. P_{v} and P_{c} are the vapour and capillary pressure. Most of the time the thermal diffusion is ignored. The vapour flux can also be written with the vapour diffusion coefficient (D_m) and m, the mass fraction of water vapour as:

$$\boldsymbol{g}_{\mathrm{v}} = -D_m\boldsymbol{\nabla}m$$

The heat transfer is driven by the conduction flux and the latent flux, due to vapour vaporisation:

$$\boldsymbol{q}_{\mathrm{c}} = -\lambda\boldsymbol{\nabla}T,$$

$$\boldsymbol{q}_{\ell\mathrm{v}} = h_{\mathrm{v}}\boldsymbol{g}_{\mathrm{v}} + h_{\ell}\boldsymbol{g}_{\ell}.$$

where λ is the thermal conductivity that could vary with temperature and the position within the material, h_{v} the water sorption enthalpy, to be often assumed equal to the latent heat of evaporation of water, L_{v}. Interested readers may refer to [22, 23, 24] for a complete demonstration of these equations. Moreover, for multi-layered walls, the contact between each layer is in general assumed to be perfect.

At the interface Γ of the material with the surrounding air, conservation of the heat and moisture flow is assumed:

$$\boldsymbol{g}_{\mathrm{v}}\big|_{x\in\Gamma} + \boldsymbol{g}_{\ell}\big|_{x\in\Gamma} = \beta\,(P_{\mathrm{v}} - P_{\mathrm{va}})\cdot\boldsymbol{n} + \boldsymbol{g}_{\infty}, \tag{4a}$$

$$\boldsymbol{q}_{\mathrm{c}}\big|_{x\in\Gamma} + \boldsymbol{q}_{\ell\mathrm{v}}\big|_{x\in\Gamma} = \alpha\,(T - T_{\mathrm{a}})\cdot\boldsymbol{n} + \boldsymbol{q}_{\infty} + \beta\,h_{\mathrm{v}}(P_{\mathrm{v}} - P_{\mathrm{va}})\cdot\boldsymbol{n} + c_{\ell}\,T_{\mathrm{a}}\,\boldsymbol{g}_{\infty}. \tag{4b}$$

where subscript a stands for the ambient air in contact with the porous material, β and α are the convective vapour and heat transfer coefficients considered as constant in the modelling exercise. c_{ℓ} is the liquid water heat capacity at constant pressure. The subscript ∞ designates the flow (mass and heat) away from the material.

2.5 Measurement of material properties

To predict the changes in relative humidity and moisture content within a material using Eq. (1a), transport and storage coefficients are needed. They have to be estimated by experimental characterisation methods. The left term of the equation of mass conservation Eq. (1a) is the moisture storage term. It can be written as:

$$\frac{\partial w}{\partial t} = \frac{\partial w}{\partial \phi}\frac{\partial \phi}{\partial t}$$

where ϕ is the relative humidity.

The moisture storage within material depends on the moisture capacity, $\xi = \frac{\partial w}{\partial \phi}$, which can be defined as the slope of the sorption isotherm curve, $w = f(\phi)$. The storage function or sorption isotherm curve is assessed by measuring the equilibrium weight of a sample exposed to successive steps of ambient air relative humidity in isothermal conditions. This method is called the gravimetric method (ISO 12571, 2013); others characterisation methods can be used [25]. Material samples are successively placed in different relative humidity conditions controlled by salt solutions. The equilibrium mass uptake is then measured at each point. These methods are highly time-consuming, because several points are required to draw a sorption isotherm curve, each of which may only reach equilibrium after several weeks.

The diffusion processes (water vapour, liquid water, gas) in material are influenced by the permeability value. The general method to measure this property is to expose the material to a pressure gradient (vapour pressure, liquid pressure or total pressure) and to measure to resulting flow. The permeability is the proportionality coefficient between the two. Each property has to be measured separately by avoiding the other pressure gradients or making them negligible. As for the sorption isotherm, this method is a steady-state method.

For vapour permeability, (δ_{v}), the most common measurement procedure is the cup method, following the standard (ISO 12572, 2013 [26]). The vapour pressure gradient is created by a difference of relative humidity between the two sides of the sample assuming constant temperature. The mass variation is measured to know the mass flow. Its principle is to measure a steady mass variation under a controlled vapour flow driven by a difference of relative humidity between the two sides of the sample under constant temperature.

The mass uptake or decrease of the whole cup is then related to the vapour permeability of the sample. From Eq. (2a), with constant temperature, in case vapour permeability is independent of vapour pressure, we can deduce:

$$g_v = \delta_{\mathrm{v}}.\frac{\Delta P_v}{\Delta x}$$

In addition, the mass flow can be expressed as:

$$g_v = \frac{\Delta m}{\Delta t.A}$$

Therefore, the vapour permeability is calculated as:

$$\delta_{\mathrm{v}} = \frac{\Delta m.e}{\Delta t.\Delta P_v.A}$$

with g_v the mass flow rate in $kg/m^2/s$, Δm is the mass uptake, Δt the time of the experiment (defined in Figure 4) and A the exposed surface of the material. Δx is the sample thickness and ΔP_v is the difference of vapour pressure between the two sides of the sample.

With vapour permeability, the vapour resistance factor μ is defined as the ratio of water vapour permeability in the air $\delta_{v,a}$ and that in the material δ_{v}: $\mu = \frac{\delta_{v,a}}{\delta_v}$.

Since the vapour permeability is moisture-dependent, a dry and wet cup experiment can be carried out with different relative humidity levels. This test is standard and widely used, as noted in the following studies [27, 20, 28, 29, 30] among others. Other methods can be used to measure moisture diffusivity [31], but they are less used because they require that the diffusion equation solution be expressed [32].

2.6 Comparison of results

In most of the studies, the numerical and experimental results were compared by comparing only the trend of the two curves. This type of qualitative comparison was made, for example, in [33, 34, 35, 36, 37].

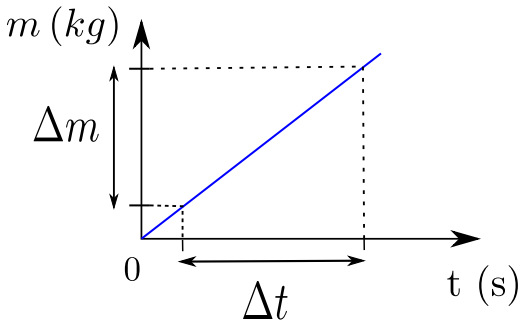

Figure 4: Results obtained with standard test to measure vapour permeability [26]

To extend the investigations and to conclude on the agreement between the two, it is important to compute the residual or relative error:

$$\epsilon = \sqrt{\int \frac{(u_{\text{observed}}(x,t) - u_{\text{predicted}}(x,t))^2}{u_{\text{predicted}}(x,t)^2} dt}\,.$$

It is important to compare this quantity ϵ to the global measurement uncertainty. The latter should not include only the sensor uncertainties, but also the other uncertainties stemming from the experimental design (sensor location, contact resistance, etc.), due to the boundary conditions (their measurement and their hypothesis), the input material properties of the model and the model itself. In other words, all the biases, illustrated in Figure 1 and analysed in the discussion, should be analysed. Their impact on the numerical results and the experimental data should be evaluated to provide a precise discussion on the validity of the comparison.

As said above, it is important to consider the uncertainty with the measurement with the propagation of uncertainties. Therefore, after the experiment, the measured field u is expressed as: $u(x,t) = u_{measured} \pm \Delta u$. The value of the uncertainty Δu will have an importance for the agreement with the numerical study. The difference between measurement and simulation has to be compared to this value using error bars for example [21]. The agreement can be considered as "good" when the deviations are within the uncertainty. This evaluation is difficult and is not always in the presented studies.

In the present review, to more accurately compare the deviations in the research reported and analysed here, we tried to quantify the agreement between measurement and simulation using the results available in the articles. We therefore measured and calculated the slope of both curves and compared them as was done in [38]. This translates a difference in the dynamic of the predicted transfer [33, 39, 40, 27, 37]. Moreover, to evaluate the deviations in the transient state, it is possible to evaluate the delay in the curve between the experiment and the modelling exercise [41, 35, 42, 34].

To quantify a difference in the steady-state, we directly measured the difference in the values on the curves [37]. Nevertheless, in most of the studies, this quantification had already been made [28, 43, 44, 20, 15, 45].

3 Literature review

The hygrothermal behaviour of hygroscopic materials obtained experimentally with the set-up described in Figure 3 can be compared to numerical simulations for different boundary conditions and at different scales e.g. the wall and material scale. This part presents an overview of this comparison. The experimental and numerical inputs will be described and highlighted according to Figure 1. If this is not the case in the paper reported, we will attempt to detail and quantify the comparison for temperature and moisture variables. At the end of each part, the summary of the main characteristics of the studies is given.

3.1 Material scale

Here we describe the studies conducted at the material scale where the characteristic size of samples is a few centimeters in the three dimensions. The boundary conditions in the experimental part can be controlled with two kinds of experimental facility: the climatic chamber and the air tunnel, as illustrated in Figure 3.

3.1.1 Climatic chamber

The boundary conditions, temperature and relative humidity, can be controlled using a climatic chamber. This facility allows one to test materials under non-cyclic or cyclic conditions with changes in temperature and/or relative humidity.

In this part, 12 studies using a climatic chamber to control experimental boundary conditions are reported [33, 39, 46, 47, 34, 38, 48, 49, 35, 42, 50, 51]. Various building materials were characterised under different loads. We can distinguish two types of boundary conditions: time-invariant (temperature or relative humidity gradient, relative humidity step) and variable conditions (climatic weather, cycle).

Non-cyclic temperature and/or relative humidity conditions
Several tests for different materials under step-wise variations of relative humidity are reported in the literature.

The non-cyclic conditions used to test materials can be temperature or relative humidity gradients between two climatic chambers. The hygrothermal behaviour of several cylindrical *lime-cement mortar* samples subjected temperature and relative humidity gradients between two climatic chambers was studied in [33, 39]. The temperature within the samples was monitored, and the moisture ratio of the samples was determined by weighing. A model including vapour diffusion and liquid flow presented good agreement for temperature within the sample but a slower than measured moisture diffusion. This was highlighted by a higher slope in the moisture variation in the material thickness, w = f(x) (for example: $250\,\mathsf{kg/m^3/m}$ for measurement versus $200\,\mathsf{kg/m^3/m}$ for simulation after 2 weeks).

In other studies [46, 47, 34, 38], samples were exposed to a relative humidity step in isothermal conditions. In all these experiments, the samples studied were sealed with aluminium tape on the bottom and lateral surfaces: only the top surface was open to moisture exchange.

In [46], experimental measurements, carried out on *cement* samples, were compared to phenomenological, based on "ink bottle effect", (Mualem [52]) and empirical (Rubin [53]) modelling of hysteresis based on classical equations. The experiment consists in applying a relative humidity step to samples, drying at 53.5% and and wetting at 97% relative humidity. The agreement was good for the comparison, even if there were more differences for the more porous *cement* samples. The simulation with Mualem's model gave the best results, a conclusion that was also found by other authors [35] and [42] with other material (*hemp concrete*) and boundary conditions.

The experimental results of the drying experiment on the *lime-hemp* material were compared with a simulation obtained with `WUFI` [34]. The cylindrical samples $19\,\mathsf{cm}$ in diameter and $3.4\,\mathsf{cm}$ thick were first wetted and than dried at a temperature of $23\,^\circ\mathsf{C}$ and 65% relative humidity. The main hygrothermal properties were measured at IBP Fraunhofer [54]. Using the default value of the liquid transfer coefficient, the drying was faster in the experiments, the delay between numerical and experimental results is of four days. A new liquid transfer coefficient, determined by fitting the adsorption experimental results obtained with the nuclear magnetic resonance method, provides good agreement between simulation and measurements; however, this value has no physical meaning.

Perré et al. [47] had a similar approach to Evrard and Herde's [34]. The value of moisture diffusivity was determined by fitting the experimental results using an inverse method. The physical model was based on the `Transpore` software [55], modelling vapour, liquid and air in the material. In this study *fibreboard* and *spruce* were investigated measuring relative humidity at the bottom of

the sample, whereas the relative humidity step was applied at the top of sample. Good agreement was obtained for spruce, but for *fibreboard*, the dimensionless diffusivity identified was non-physical (> 1). According to the authors, the deviations could be explained by a non-Fickian behaviour with a dual-scale character of mass diffusion in this kind of material.

Busser et al. [38] used the same kind of experiment as [47] but measuring the relative humidity diffusion in material with sensors at different depths in *wood fibre insulation* samples. In addition, the mass gain was measured by weighing samples regularly. The results were compared to numerical data obtained with `WUFI` software modelling vapour and liquid water transport. The material properties used were measured by several laboratories using steady-state methods during an earlier French project: Hygro-Bat [56]. Comparing the results showed that, for the mass change, the overall behaviour was adequately described by simulation, but the code under-estimated the relative humidity dynamic in the transient state: the slope of the curve was lower. The authors explain these differences with the materials' properties. An error in the sorption isotherm can explain the difference of the steady-state value observed for the mass change. These experimental data [38] were used to determine adapted material properties using an inverse method [57]. The new value of vapour permeability identified was non-physical and very different from the value measured with traditional cup methods. According to the authors, this indicates that the standard model did not correctly represent the phenomena involved.

Cyclic moisture conditions

The material can be tested under cyclic conditions. Often only one face of the sample is open to ambient air and the others are sealed.

In the study proposed by Van Belleghem et al. [48] a hygrothermal model was combined with computational fluid dynamics (CFD) resulting in a so-called "CFD-HAM" model. The results obtained with this model were compared with a moisture buffering value (MBV) experiment between 50% and 70% relative humidity on *calcium silicate* (CaSi). The relative humidity and temperature were monitored with sensors at different depths. The material properties were measured by different laboratories during the HAMSTAD project [58, 59]. The CFD-HAM model computes the water vapour transport in the hygroscopic material as well as in the surrounding air. The comparison between model and experiment showed a greater difference than uncertainties: $\pm 4\%$ compared to a sensor accuracy of 1.4% relative humidity. The model underestimates the relative humidity amplitude. The agreement was better for sensors near the surface of the material. The comparison for temperature showed good agreement: the difference was lower than $0.2\,°\mathrm{C}$. The uncertainties in the moisture dependence of materials' properties could explain the deviations observed.

The *lime-hemp concrete* material characterised by [34] was used in [49] to compare measurements and simulations obtained with two models: `WUFI` software and another model based on Eq. (1) implemented in `COMSOL`. The models provided similar results with an over-evaluation of the mass change during the MBV experiment: a 10% difference. Moreover, the temperature prediction differed by $0.25°C$ between measurement and simulation. Differences were greater for the `WUFI` simulation. The initial slope during the relative humidity change was accurately predicted by the models.

Hemp concrete was studied in [35] and [42] with a numerical model implemented in `COMSOL` software. In these two studies, hysteresis was taken into account: Mualem's phenomenological model and Pedersen's empirical [52, 60] model. The results confirm that Mualem's hysteretic model gave a overall better agreement. During the cyclic test, only the top surface of the material was exposed to the change in the air's relative humidity. The temperature and relative humidity were monitored at different positions within the sample and the overall mass variations were continuously measured. The comparison between experimental results and simulation for sprayed hemp concrete [35] and coated hemp concrete [42] showed that measurements vary faster than prediction for relative humidity. As before, the deviations increased deeper in the material. A change in hygric properties can improve the comparison (see Table 5). To represent the experimental results more accurately the influence of temperature on the sorption isotherm was taken into account [51, 61]. The agreement was improved

even if some differences remained with variable temperature conditions: there was a 1.% difference in relative humidity and of 2% for the moisture content.

In [62] Zhang et al. exposed a *spruce* plank to a dynamic moisture response test: three stepwise temperature variations under constant relative humidity (80%), six stepwise relative humidity variations (three over 16h and three over 8h) under constant temperature (50 °C); the same steps were repeated at 23 °C. The samples were weighed with a scale during the experiment. Four models were developed in Modelica language [50] to predict these results on *spruce* material. As in [51] the model taking into account temperature-dependent hysteresis seems to capture the general trend of mass variations better even if all the modelling results deviated from the measurement (maximum deviation, 1.5% of moisture content).

3.1.2 Air tunnel

The literature reports several studies conducted in an air channel using two test facilities: the Transient Moisture Transfer (TMT) test facility [29] and a double climatic chamber with an air inlet over the sample [48]. In these experiments conducted on different materials, temperature and relative humidity sensors are placed at different depths in the material to measure the diffusion process. Moisture accumulation is measured with gravimetric load or a precision scale. Only the top surface of the sample is open to moisture transfers. The results obtained with these experiments are compared to those obtained with simulation tools.

The results obtained with the `HAM-Tools` software [63] were compared with experimental results obtained by Talukdar et al. [29] on samples of *spruce plywood* and *cellulose insulation* with data from [64]. The samples were subjected to a relative humidity step and cyclic conditions of air relative humidity. The liquid and vapour phases were modelled [45]. The results were similar for both materials with greater errors for cellulose. The differences were greater with oscillating boundary conditions (0.7% versus 0.35% relative humidity), even if they remained within the experimental uncertainty ±1%. Nevertheless, the moisture accumulation kinetics seems to be under-predicted by simulation. For cellulose insulation, the predicted variations of relative humidity were slower than with the measurements.

Gypsum board behaviour was investigated in [21] with simulations carried out by 11 participants. Simulations were compared to experimental data on coated (acrylic and latex paint) and uncoated gypsum boards subjected to a relative humidity step for a 24-h period each (30%-70%-30%) performed at constant temperature. All the results showed the same behaviour: no simulation tool was better than the others in predicting the measurements. For uncoated gypsum, the experimental data showed a faster transition for relative humidity (2 h) and moisture accumulation. The results were under-predicted (by 5%) for relative humidity. The errors were lesser for temperature (0.5 °C). The comparison of vapour pressure gave better agreement than relative humidity because it took temperature into account. The uncertainties in the material properties used in the models (vapour permeability, sorption isotherm) were pointed out by the authors to explain the deviations.

The TMT facility increased the impact of the heat and mass convective transfers with the presence of airflow. Therefore, the combined CFD-HAM model was adapted to solve equations in the entire domain (air + material). In Steeman et al. [65], the authors implemented heat and moisture transfer equations in `Fluent` CFD software [66]. Hysteresis was included in the CFD solver using the above-mentioned model developed by Mualem [52]. Experiments carried out on *gypsum* showed that the equilibrium level was not well predicted by this model [65] for *uncoated gypsum*; the difference was greater than the uncertainty of sensor (2% relative humidity). Good results were obtained with coated gypsum. Then the model was adjusted to account for liquid transfer and simulate the drying behaviour of the saturated sample (the same as the one used in [48]) with a conditioned air flow on the top [67]. The shape of the drying curve was satisfactorily predicted by the simulation, even if the slope was higher in the measurements. The capillary effect observed in temperature measurements was reproduced correctly.

The same experimental study was carried out on a *ceramic brick* [68]. The 3D simulation was

based on material properties from the literature [69]. The heat and mass convective coefficients were determined with the CFD simulation [70]. For the temperature, the agreement in the insulation material around the sample remained within the predefined uncertainty (0.1 °C); this was not the case within the material (0.3 °C difference and a delay in the temperature increase). The difference was greater near the surface. The mass loss curve was over-estimated by more than 10% of the variation of the moisture content value in the second part of the drying, higher than the uncertainty (4% of the value). The drying rate was also high [70]. The moisture content distribution in the ceramic brick over time, measured using the neutron radiography method, showed a slower decrease of the moisture content compared to the simulation, and the difference increased with time.

3.1.3 Summary

Table 1 gathers characteristics (the phenomena considered, the type of experiment) of all the studies reported in the "Material scale" section.

The effect of temperature on the sorption isotherm is taken into account in some studies, noted in Table 1 with the number [1] when hysteresis was involved.

	Model: terms taken into account					Experiment			Measurement			
Ref	Hysteresis	Vapour	Liquid	Air	Thermal diffusion	Non-cyclic	Cyclic	Real	Relative humidity	Mass	Temperature	Material
[33] [39]		x	x		x	x				x	x	Lime-cement mortar
[46]	x	x	x			x				x		Three cement samples with different water-to-cement ratios
[34]		x	x			x				x		Lime-hemp
[47]		x	x	x		x			x		x	Spruce, wood fibre
[38]		x	x			x			x	x	x	Wood fibre
[48]		x					x		x		x	Calcium silicate
[35] [42]	x	x	x				x		x	x	x	Sprayed and coated hemp concrete
[51]	x [1]	x	x				x		x	x	x	Sprayed and coated hemp concrete
[49]		x	x				x			x		Lime-hemp concrete
[62]	x [1]	x					x			x		Spruce
[21]	NA	x	x	x			x		x	x	x	Coated and uncoated gypsum board
[45]		x	x				x		x	x	x	Spruce plywood and cellulose insulation
[65]	x	x	x				x		x		x	Coated and uncoated gypsum board
[67]		x	x			x			x	x	x	Calcium silicate
[70] [68]	x	x	x			x				x	x	Ceramic brick

Table 1: Summary of reported studied at material scale

3.2 Wall scale

The models can also be validated using experimental data within test walls, i.e. the characteristic sizes of samples are 1 m*1 m*10 cm. The walls can be exposed to controlled conditions in climatic chambers or to outdoor conditions on one side. The aim of these studies was to measure and control the transfers through the wall and obtain the moisture profile within the wall. The accuracy and prediction of the models were assessed by comparing results with experiments. Different wall compositions were tested to investigate the impact on the validation process.

3.2.1 Controlled conditions

In these studies, walls were studied experimentally by placing them between two climatic chambers controlled for temperature and relative humidity. In each chamber, the boundary conditions can be constant or variable.

Mono-layer
For example, a model based on the Umidus model [71] was implemented in the `Spark` simulation environment [72]. The results obtained with this model were compared with experimental data given by [73] where a *hemp concrete* wall was placed in a biclimatic chamber. The "indoor" boundary conditions were constant (23 °C, 50%), while the "outdoor" conditions varied (23 °C to 32 °C and 50%-30%). The relative humidity and temperature were monitored within the wall and in the centre of each room. The transient moisture behaviour of hemp concrete was difficult to model with varying conditions, a 2.4% difference in relative humidity is observed. This deviation is greater than the sensor uncertainty, whereas the temperature results were accurately represented (the difference is less than the experimental uncertainty (0.5 °C)) [72]. Sprayed hemp concrete was also studied with the same test facility [35]. The temperature amplitude and kinetics were well predicted by the hysteretic model, whereas relative humidity measurements were faster in desorption than the simulation. Nevertheless, the error was less than 1% relative humidity. Similar to previously discussed studies at the material scale, the agreement was better at the wall surface.

In [74] the behaviour of the *hemp concrete* wall was compared to a model that took into account the effect of temperature on the sorption isotherm curve using Milly's model. The results showed that the non-isotherm model results in significantly better prediction of the relative humidity variation in the tested wall. The maximum difference was 3% for relative humidity compared to 1.5% sensor uncertainty. According to the authors, the temperature variation was satisfactorily predicted even if a maximum difference of several degrees was noted.

Another model developed with `COMSOL` without hysteresis but with the same modelled phenomena was used to simulate the hygrothermal behaviour of a *hemp concrete* wall in [75]. The specimen was placed between two climatic chambers and subjected to a relative humidity step with or without a temperature gradient. The model seems to over-estimate the heat flow and the temperature variations while it tends to under-estimate the variations in relative humidity at the middle of the sample. The slope of relative humidity variation was lower for the simulation: 1.5%RH/day versus 12%RH/day for measurements.

In [76] Slimani developed a model based on `HAMFitPlus` [77], using three conservation equations written with temperature, absolute humidity and air pressure as potentials. This model was validated according to different controlled boundary conditions (isothermal, non-isothermal and cyclic conditions) applied to a *wood fibre* wall located between two small rooms, both controlled in temperature and relative humidity by saturated salt solutions. Temperature and relative humidity were measured in both chambers, at the surface of the wall and within the wall. The deviations between model and measurements increased for non-isothermal and cyclic conditions compared to the isothermal condition. With isothermal conditions, the gap (0.1 °C for temperature, 1% for humidity) was lower than uncertainty (0.2 °C and 2%). In the transient case, the relative humidity and temperature kinetics were not well predicted: the predicted relative humidity was slower than the measurements and/or

damped by 4% and the temperature was damped by 0.5 °C) compared to the measurements. The author says that these deviations were linked to over-estimations of moisture capacity resulting from the local-equilibrium hypothesis. According to the author, this assumption had to be reconsidered in the establishment of the conservation equation.

To investigate the role of the interior finishing, an experiment was conducted on a two-storey test facility with two identical rooms [15]. Two surfaces of each room were covered with the material investigated: *wood* panelling or *uncoated gypsum* board, depending on the room. The moisture content of the interior finishing, measured with electric resistive probes, was compared to `WUFI` simulations. Two different moisture load profiles were applied: 100 g/h moisture generation for 10 h followed by 14 h without moisture generation, and 200 g/h moisture generation for 2 h followed by 22 h without moisture generation. The material's properties were obtained with classical measurements. The agreement was better during moisture generation than the free-floating evolution. Moreover, the agreement was better with gypsum board than wood panelling, especially in terms of the desorption kinetics.

Medjelekh et al. [78] studied unfired clay masonry experimentally and numerically. The heat and moisture model were implemented in Cast3M software [79] with the finite element method. In the model, an "apparent vapour permeability" was defined by taking into account both vapour and adsorbed liquid film diffusions. Moreover, hysteresis was modelled with Merakeb's model [80], initially developed for wood material. The material properties (sorption isotherms, thermal conductivity and apparent vapour permeability) used were measured at the material scale, on the same material. The permeability value was obtained using an inverse method from the kinetics of the moisture mass variations in the samples. Then the numerical results were compared to measurements at the wall scale. The boundary conditions were controlled with two climatic chambers and the wall was monitored with thermo-hygrometers. The wall was first exposed to drying conditions and then to cyclic of relative humidity. In both cases, the agreement between the experimental and numerical results were good: the difference was lower than 1.25% for relative humidity compared to 1.8% for the sensor uncertainty, and lower than $0.25°C$ for temperature (uncertainty, $0.4°C$).

Multi-layer

This part investigates the walls composed of several layers, as are found in real walls. The problems modelling and comparing different walls increased. In the literature the wall samples are mainly studied with two types of test facilities.

In the first one, the walls are exposed to controlled conditions on both sides. For example, *timber* walls with insulation were studied using the test facility described in [81]. The wall, located between two climatic chambers, was successively exposed to permanent conditions (winter) and dynamic loads. The experimental results were compared to the simulations with `BuildingPore` and `WUFI` software [82]. The material properties used in the codes were measured on samples used in the experiment. Both software programs showed that the differences were greater within the wood than in the insulation material and that the moisture transfers were faster in the experiment than in the code predictions. The authors suggested that an increase in the diffusion coefficient value used in the simulation could improve the agreement between measurement and simulation.

Kalamees and Vinha compared the results of several tools (`1D-HAM` [83], `MATCH` [84] and `WUFI-2D`) with experimental tests [20]. The test equipment was composed of a wall located between two chambers simulating two different climatic conditions, either constant or cycling. The wall structures were composed of different insulation materials (*mineral wool*, *cellulose insulation* and *sawdust insulation*), a vapour barrier (plastic sheet or bitumen paper) and sheathing. Measurements of all the properties of the materials used were taken (thermal conductivity, permeability, density, moisture storage function). Three walls were presented in detail in [85]. The predictions of all three software programs were close for all test wood-frame walls. The differences were greater for cyclic conditions than stationary conditions (13% versus 5%, respectively for maximum differences for relative humidity). The authors suggest that the difficulties simulating the hygrothermal behaviour correctly with rapidly

varying boundary conditions were due to inaccurate determination of material properties. In [20] the authors also emphasised on the importance of the initial condition, especially for moisture content. In this study it was difficult to compare the results between walls and to distinguish the behaviour of hygroscopic and non-hygroscopic insulation because the type of vapour barrier differed and the interior finishing influenced the results. Additional investigations of wall assemblies with vapour-tight sheathings were also conducted in [85]. The drying experiment carried out showed that the consideration of the capillary flow improved the results for high relative humidity ($> 90\%$), but has a lesser influence for non-hygroscopic insulation (fibreglass) as well as for the transfer dynamics, still under-estimated.

The second test facility is a full-scale test hut composed of two identical test rooms, one on top of the other, assembled inside a large-scale environmental chamber [86]. The moisture buffering effect of the material was studied in this two-storey test hut [15], as described above. This facility was also used to validate `HAM-BE`, a code developed on `COMSOL` [87]. Classical heat and mass transfer mechanisms were modelled (conduction and convection of sensible and latent heat, vapour diffusion, liquid flow and air convection). The material properties used in the code were derived from laboratory measurements. *Wood-frame* walls with *glass wool insulation*, *painted gypsum boards*, cladding and sheathing were exposed to wetting and drying conditions. A water tray was therefore added in the wall and used as a moisture source. The moisture content of the sheathing was measured at different positions within the wall with gravimetric samples. The prediction generally matched the experimental data closely, but we can observe deviations depending on the configuration. The agreement was better with oriented strand board (OSB) as sheathing than with plywood. Moreover, the agreement was also better when a vapour barrier was present, reducing the impact of mass transfer. The authors attributed the discrepancies between experiment and numerical modelling to: the anisotropy of materials properties, the moisture content measurement process, which could produce air leakages and disturb the experimental conditions and the imperfect control of boundary conditions.

3.2.2 Outdoor condtions

The following studies considered walls subjected to real conditions on one side. The other side is exposed to controlled climatic conditions that can be constant or variable. As above, the wall composed of a single material and the multi-layered wall were distinguished.

Mono-layer

In this part, only mono-layer walls were considered. To compare with numerical results, the temperature and relative humidity are measured within the wall to investigate hygrothermal profiles.

The hygrothermal behaviour of three materials: *aerated autoclaved concrete*, *hemp lime concrete* and *vertically perforated brick* was studied experimentally in [37]. The experiment placed walls between a climatic box and the laboratory room. In the climatic chamber, constant or cyclic of temperature and relative humidity conditions were created. The temperature and the relative humidity were recorded in the middle of the wall, at each surface (indoor and outdoor), in the climatic chamber and the laboratory room. The moisture adsorption of the wall was measured with two samples of materials placed on a scale at each side of the wall. For the vertically perforated brick, only the heat transfer model by conduction was needed to simulate the behaviour, and the model and the measurements were in good agreement. For the aerated autoclaved concrete and hemp lime concrete, a heat, air and moisture model based on [22] was implemented in `COMSOL`. The relative humidity variations were underpredicted, especially in the cyclic experiment and for uncoated hemp lime concrete (slope: $2.66\,\%/\mathrm{h}$ for measurements and $0.4\,\%/\mathrm{h}$ for simulation). If the hemp concrete was coated, the model prediction was closer to the measurements even if a small, 1-h gap remained, similar to the study reported in [42]. Concerning the aerated concrete, the results presented a water vapour redistribution that was much smaller (9%) and mostly slower (2 h) than the experimental results, because the diffusion coefficient was assumed to be constant. In the cyclic condition, the daily variations of relative humidity were not represented. The authors explained that the sorption hysteresis and the moisture dependence of the properties had to be taken into account to improve the simulation.

Tariku et al. [88] compared a field experiment on a test house with an aerated concrete wall and simulation with the 2D version of `hygIRC` software [89]. The material properties used in the model were based on the literature or on the software database. The indoor temperature and relative humidity were monitored and controlled (23 °C and 45%). Three temperature and relative humidity sensors were placed at different depths in the wall. The measurements were slightly more sensitive to weather changes than the simulation, causing a phase shift and a difference in amplitude at some peaks. The material properties, not measured, may not have represented the material used, which can explain the deviations observed.

In [27] *wood fibre* walls were tested under different internal and external conditions on PASSYS rotating cells with a controlled indoor environment. The properties of materials used were measured with classical methods by several laboratories [56]. A numerical model was developed on `DYMOLA` software taking into account the vapour diffusion and liquid transfer [27]. The comparison with the measurements showed a good correlation for the temperature measurements, but differed for moisture. The simulations did not reproduce the daily dynamics of relative humidity and underestimate the overall variation (slope: 5.5 %/day for measurement, 3.75 %/h for simulation). Moreover, the relative humidity equilibrium value was under-predicted by 5% in the simulation, whereas the sensor uncertainty was 2% for relative humidity. A change in material property values partially improved the level of agreement (see also Table 5).

In his thesis, Raji [90] studied *plain wood* walls with in situ experiments on *cross-laminated timber* (CLT) building panels. To measure the properties of the wood material used (density, conductivity, specific heat, diffusion coefficient, air permeability, sorption isotherm), laboratory measurements were taken on the same timber samples. A model, based on the assumptions presented on [91], was developed in `COMSOL`. Then energy and mass conservation were partially decoupled: enthalpy transfers due to the water content gradient were ignored compared to this, driven by the temperature gradient. More deviations were observed with the second model (error, 7% in relative humidity versus 3%). The overall shape was adequately determined, with an over-estimation of the average moisture content value (6% amplitude) and a lower daily variation and sensitivity to a moisture change compared to the experimental data.

Multi-layer

Similar types of study were conducted with more complex walls here; the temperature and relative humidity were measured within the wall mainly at the interfaces of different layers. In the following studies, the walls were tested in field experiments with a test house.

A *wooden-frame* test house exposed to natural outdoor conditions [92] was used to compare results with a numerical study conducted with `HAM-Tools` [93]. The walls were composed of wood studs with *fibreglass insulation* and *OSB* as interior finishing. Several configurations were studied: walls with and without a vapour-barrier, indoor climate with and without heating, humidification and mechanical ventilation. The response of the wall to a slow change in relative humidity with a daily temperature variation was sufficiently reproduced by the simulation. With abrupt temperature changes, the wall's behaviour under a relative humidity change was not reproduced correctly: a slower and lower desorption was numerically observed. According to the authors, the use of the properties determined in steady-state could explain the deviations. At the same test facility, Labat et al. [94, 28] studied two walls: one with *mineral wool* and OSB and the other composed of *wood fibre* and gypsum board as indoor siding. Each wall was subjected to vapour production and free evolution. The results showed that the case with wood fibre was more difficult to model, due to its hygrothermal properties, in particular for absolute humidity: the average difference was lower than 0.8 g_V/kg_{DryAir} for the wood fibre wall versus 0.05 g_V/kg_{DryAir} for the mineral wool wall. Temperature differences were lower than uncertainty (difference of 0.3 °C for 0.8 °C of uncertainty).

Field measurements on a test house composed of two test *wood-frame* walls with wood fibreboard as sheathing and gypsum board as interior finishing were compared with `WUFI 2D` and `1D-HAM`, as reported in [85]. Two different insulation materials, *cellulose* and *glass wool*, were used. Simulations

provided good agreement for temperature but slower dynamics for relative humidity. The phase shift seems to be lower for the glass wool.

A concrete wall covered with *aerogel rendering* was studied in [95]. The indoor conditions were controlled. The temperature and relative humidity were monitored during free evolution in summer. The `WUFI-Pro` software predictions were not within the sensors' accuracy: the maximum deviation for the temperature at the interface between the rendering and the concrete was 0.6°C and 2-6% under-estimation for relative humidity. The same orders of magnitude were obtained in [96] for *aerogel-based* and *perlite-based* insulation used to retrofit in-situ walls.

3.2.3 Drying

When a building is exposed to rain, the wall's ability to release moisture should be known in order to prevent moisture damage. Therefore, the wall's behaviour is studied during drying to assess its performance in terms of the drying rate, a crucial parameter in this context. In reality, walls are exposed to the climate conditions at the exterior side with varying temperature and relative humidity at daily and yearly scales. Indoors, the impact of occupants also leads to variable conditions.

Drying experiments were carried out with pre-wetted materials or walls to simulate rain wetting with the boundary conditions of drying constant or variable (cycles or real conditions).

To simulate rain infiltration in a typical Canadian residential *wood-frame* construction, a piece of pre-wetted wood was inserted on the test wall's bottom plate [97]. The test assemblies form the walls of a test hut built within a climatic chamber where the sinusoidal variations of outdoor climate conditions were simulated. The moisture content of the bottom plate was measured. Comparing the bottom plate response with `WUFI-2D` simulation, we observed a lower simulated drying rate for all wall assemblies. The decrease of the vapour diffusion resistance factor value of the fibreglass improved the comparison. Nevertheless, a number of discrepancies remained, and can be explained by the uncertainties on the initial conditions and the material properties. The response of the building facade to wind-driven rain was also studied in a full-scale test to assess the influence of this boundary condition on HAM transfer models [98]. The traditional approach was questioned because the weight change was overestimated by the model.

Drying experiments under variable conditions on *OSB* alone and on OSB with water-resistive barrier were presented in [99]. Initially the OSB specimens were immersed in a water bath for several days. During the test, the mass of the wall assembly components was monitored with load cells [100]. The moisture content was compared to the results obtained with `HygIRC` software. The software used the hygrothermal properties of materials derived from tests on small-scale specimens undertaken in the laboratory. The comparison showed that the moisture content is predicted with a 5% error, whereas the weighing system was able to discern a 0.125% change of moisture content [100]. Moreover, in the first 4 days, for OSB alone the decrease of moisture was faster by a half-day in the measurements. With coated OSB, predictions were faster. According to the authors, the drying was controlled by liquid permeability, and a change these properties could improve comparison.

The temperature-driven inward vapour diffusion (also called thermal diffusion, Eq. (2a)) in a multi-layered wall, initially wetted, was studied experimentally [36]. Different configurations were tested. The drying experiment was carried out with constant or daily cyclic conditions at the exterior side (outdoor 40 °C for 8 h and 19 °C for 16 h). The mass was measured with a scale, while temperature and relative humidity were monitored at different depths in the assemblies. A model based on classical assumptions and described in [40] was able to reproduce the variations of the total mass correctly during the drying but less during the wetting period. The drying slope was under-estimated, especially for cyclic conditions ($-1.17\,\mathsf{kg/m^3/day}$ for the simulation and $-2.06\,\mathsf{kg/m^3/day}$ for the measurement). Moreover, it was important to note that, in this study, the convective transport coefficients were fitted to obtain the best agreement but they have no real meaning. Nevertheless, according to the authors, the agreement was good, the difference between simulation and measurements was less than 20%, so the temperature-driven moisture transport was accurately described. THe difference can be explained by properties' uncertainties and by the fact that the hygrothermal behaviour on a layer was influenced

by the behaviour and properties of surrounding layers.

In addition, field experiments were used to study the drying of *CLT* panels in [44] and [43]. McClung et al. [44] showed that the drying behaviour of a CLT wall assembly was much more significantly influenced by the wall design than by the wood species. The comparison of experimental results with the simulation (`WUFI` [44] and `DELPHIN5` [43]) showed that the deviations were the greatest at the centre of the panels, reaching more than 3% of the moisture content. The differences can be explained by the lack of precision of the initial conditions and the material's properties. The parameter study conducted by the authors showed that here, the parameters with the greatest impact depend on the wall's configuration [43] (see Table 5).

The drying behaviour of *light concrete hollow brick* structures exposed to outdoor conditions on one side was studied in [41]. The indoor side was controlled. The numerical model, based on the `Philip and De Vries` theory [91] was coupled with an experiment design optimisation to determine the optimal parameters fitting the experimental results. The model gave good results modelling the cavity of concrete brick: the same equilibrium value and good drying time. Nevertheless, the agreement depends on the position observed in the brick.

3.2.4 Summary

Table 2 gathers various details (the phenomena considered, type of experiment) of all the studies reported in the "Wall scale" section.

The symbol * indicates that the flow (heat or mass) is also measured in the experiment. The effect of temperature on the sorption isotherm is taken into account in some studies, noted with the number 1 in the "hysteresis" condition in Table 2.

	Model: terms taken into account					Experiment			Measurement			
Ref	Hysteresis	Vapour	Liquid	Air	Thermal diffusion	Non-cyclic	Cyclic	Real	Relative humidity	Mass	Temperature	Material
[15]		x	x			x			x	x	x	Wood panelling / gypsum board
[87]		x	x	x		x				x	x	Wood-frame
[72]		x	x		x	x			x		x	Hemp concrete
[35]	x	x	x				x		x	x	x	Hemp concrete
[75]		x	x			x			x		x *	Hemp concrete
[76]		x	x	x		x	x		x *		x	Wood fibre
[82]		x	x			x	x		x		x	Timber wall + insulation
[20]		x		x		x	x		x		x	Insulation material + vapour barrier + gypsum board
[20]		x	x			x	x		x		x	Insulation material + vapour barrier + gypsum board
[85]		x	x			x	x		x		x	Same wall with more vapour tight sheathing
[37]		x	x			x	x		x	x	x	aerated autoclaved concrete, hemp lime concrete, vertically perforated brick.
[88]		x	x	x				x	x		x	Aerated concrete
[27]		x	x	x	x			x	x		x	Wood fibre
[90]		x	x					x	x		x	Wood
[93]		x	x	x				x	x		x	Wooden frame with fibreglass + OSB + exterior cladding
[94] [28]		x	x	x				x	x		x	Wooden frame with mineral wool + OSB or wood fibre + plaster

Ref	Hysteresis	Vapour	Liquid	Air	Thermal diffusion	Non-cyclic	Cyclic	Real	Relative humidity	Mass	Temperature	Material
[95]		x	x					x	x		x	Concrete + aerogel rendering
[44]		x	x			x			x	x	x	CLT panels
[43]	NA	x	x	x		x			x	x	x	CLT panels
[41]	NA	x	x			x			x		x	Light concrete hollow bricks
[101]	NA	x	x	x			x			x		OSB
[97]		x	x				x			x		Typical Canadian wood-frame constructions: gypsum, fibreglass insulation, wood-based sheathing.
[98]	NA	x	x					x		x	x	Calcium silicate
[36]		x			x		x		x	x	x	Gypsum board/ glass fibre/ OSB/ water resistive barrier/ brick veneer
[78]	x	x	x			x	x		x		x	Unfired clay
[74]	1	x	x				x		x		x	Hemp concrete

Table 2: Summary of studies reported at the wall scale

4 Discussion

This section discusses and compares the results of the studies cited in the previous section. This discussion is based on the four possible biases identified in Section 2 and illustrated in Figure 1. First, we will focus on bias b_1 concerning the experiments. The impact of the protocol design, the type of materials and the configuration of the experiments will be analysed. Then the influence of the boundary condition on both the experiments and the numerical model will be discussed (bias b_2). For bias b_3 in the model, the discussion will be organised according to the physical phenomena and the numerical resolution. Then the influence of the material properties on the numerical results is investigated (bias b_4).

4.1 Experimental parameters

4.1.1 Protocol design

During an experiment several uncertainties will impact the results on the field u measured such as relative humidity, temperature, vapour pressure, mass or overall moisture content. To obtain the overall uncertainty, the uncertainty propagation equation must be applied:

$$\Delta u \;=\; \sqrt{\sum_{i=1}^{N} \left(\frac{\partial u}{\partial p_i}\, \Delta p_i \right)^2}$$

where N is total number of uncertainties introduced in the measurement process and Δp_i is the uncertainty due to source i. Several sources can be identified in the context of the study. The first one deals with the sensor position. This uncertainty was evaluated using numerical methods in [102] and appeared to be negligible compared to the other uncertainties. It should be noted that it is rarely taken into account and its importance has to be analysed when placing sensors, particularly at the wall scale. The second one concerns the additional air resistance added when a sensor is implemented within the samples. In [38], different configurations with one, two or three sensors inside the wood fibre material were compared experimentally to validate the protocol. The results showed that cutting and reconstituting the sample to add sensors has no impact on the results. A third uncertainty comes from the assumption of one-dimensional transfer through the sample. Transfer in other directions can occur due to the airflow or material heterogeneity. This was verified in [29] by evaluating the difference in temperature and relative humidity with several sensors at the same depth in the material but at different positions in the other direction. For relative humidity, the difference was lower than 0.5%. Last, sensor accuracy is one of the most important uncertainties. Sensors have their own uncertainty given by the manufacturer. For temperature sensors such as thermocouple and capacitive sensors, the classical accuracy is better than 0.5 °C for temperature and 2% for relative humidity sensors. The balance to measure mass can be highly accurate, for example: 0.0001 g.

Most of the studies seemed to consider only the uncertainty of the sensors. Even if it is a satisfactory approximation, the importance of other uncertainties should be verified for each experiment. Moreover, before the experiment, the sensors used have to be calibrated with a reference sensor. This procedure is described in [29]. To reduce uncertainties, we can also place several sensors at the same position in the material. Nevertheless, this can disturb the measurements because the hygrothermal sensors are intrusive. To test the repeatability of the protocol, the experiment must be reproduced several times [29, 38]. If the different results are close, the protocol and the experiment data are validated and can be compared to the model prediction. These steps are not systematically reported in the articles presented, even if it is very important to avoid any biases in the comparison with numerical results.

4.1.2 Type of materials

The hygrothermal behaviour depends on the transport coefficients such as the diffusion coefficient or the storage capacity of material. The response of wood panelling and gypsum board as coatings was

compared in [15]. The results showed that the differences between model and experiment were greater for wood. This may be related to the fact that wood material has a higher moisture capacity and lower vapour permeability.

The case of spruce plywood and cellulose insulation was compared in [29]. More differences were observed with cellulose insulation. The presence of glue in plywood reduces the effect of the moisture transfers. The results with OSB and plywood sheathing were compared in [87]. The deviations were greater with plywood (see also [85]). A behaviour difference was also observed when the modelling the buffering effect of chipboard and plywood in [103]. The effects of fibres can be the source of more complex behaviour at the microscopic scale. PERRÉ ET AL. showed that wood fibreboard did not have a classical behaviour with moisture compared to spruce [47]. In this article, the value of adjusted diffusivity, f, defined as the inverse of vapour resistance factor μ, was non-physical ($f > 1$) for low-density fibreboard. This can be explained by physical phenomena occurring in wood, called the multi-scale effect, which were not modelled.

The study reported in [37] showed that the model problems representing bio-based materials, where the effects of heat, air and moisture transfers are more significant than in concrete or ceramic brick. This conclusion was confirmed by the results of [88], [78] and [3] on aerated concrete, unfired clay and ceramic, respectively. Moreover, if the hygroscopic effect of materials was reduced with coating [65] or with a vapour barrier [87], modelling was easier.

The performance of wood-frame walls with two different insulation materials and indoor sidings was compared in [28]. The wood fibre wall presented more deviations for both temperature and absolute humidity than the glass fibre wall. The hygroscopic effects were more significant in wood fibre because glass fibre is almost non-hygroscopic.

Indeed, the discrepancies seem to increase when considering bio-based materials, such as hemp concrete or wood-based material. Figure 5 compares different properties used in hygrothermal models for mineral and bio-based materials. As illustrated in Figure 5(a), the air permeability of these materials is several order of magnitude greater than mineral materials except for glass wool. Other hygrothermal properties of materials can be compared: the vapour permeability in Figure 5(b) and the moisture capacity in Figure 5(c). It can be noted that the air permeability varies greatly for bio-based materials but there is less spread in the other parameters (the vapour permeability and the slope of the sorption isotherm). Thus, as will be discussed below, the air transfer through this type of material might have an influence on the comparison.

The main conclusion is that the differences between the measurement results and modelling increase when the effect of heat, air and mass coupling increases, as with bio-based materials such as hemp concrete or wood-based material (spruce, wood fibre, cellulose). Table 3 summarises the conclusions on the comparison between measurements and simulation depending on the type of material (hygroscopic, bio-based or non-hygroscopic).

4.1.3 Configuration and scale of samples

This part investigates the comparison between the numerical study and the measurements according to the scale of study: the material and wall scales.

At the material scale, the studies compared temperature and relative humidity (T, ϕ) values at a specific location within the sample (x_0): $T_{observed} = T(x_0, t)$ and $\phi_{observed} = \phi(x_0, t)$ or compared the moisture content of the whole sample (w): $w_{observed} = w(t)$. Therefore, we can distinguish the local variables (T, ϕ) and the overall variable (w). For a local approach, sensors were placed within the material at different depths. At the wall scale, sensors were also placed inside the wall, at different depths. The moisture content of the wall or of each layer can also be measured by removing and weighing samples out of the wall.

To study the material, agreement is generally better near the surface than deeper in the material: [48] for CaSi, [21] for gypsum. The penetration depth depends on the hygrothermal properties of the material [15], and the transport inside the material is influenced by its microscopic structure [47], which is difficult to represent in a macroscopic model. For example, in bio-based material, the presence

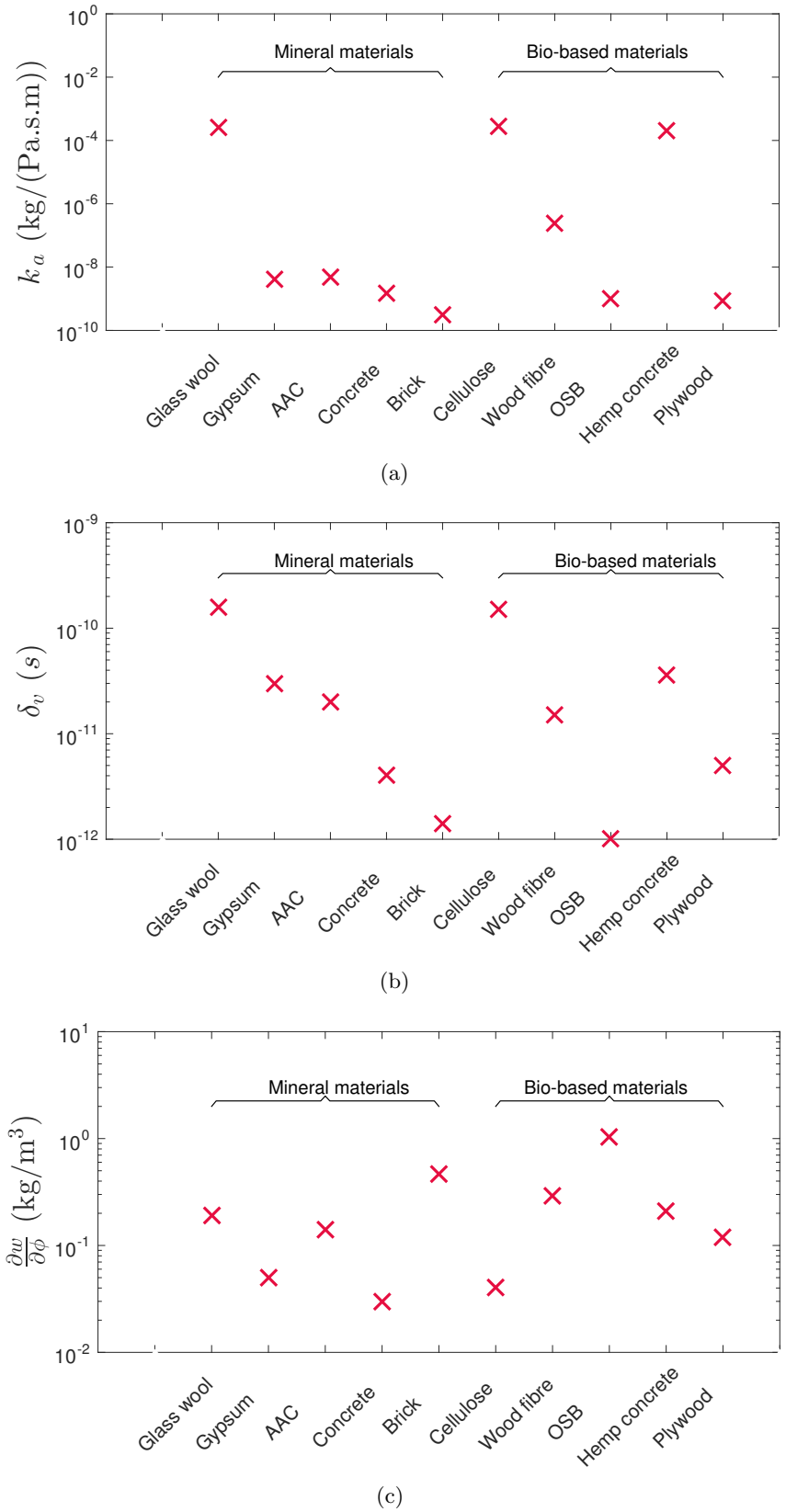

Figure 5: Air permeability (a), vapour permeability (b) and sorption capacity (c) of some materials used in the experimental investigations [104, 105]

Type of material	Example	Conclusions
Hygroscopic mineral material	Aerogel, calcium silicate, aerated autoclaved concrete, gypsum	Good agreement for temperature. The transfer kinetics is under-estimated in transient state by about 2 h. Deviations are greater with variable conditions.
Hygroscopic bio-based material	Hemp concrete, wood-based material, cellulose	Deviations for temperature prediction appear with dynamic conditions. Relative humidity kinetics is not accurately predicted, especially with varying load: difference in initial slope and equilibrium value. The adapted values of properties to fit the simulation differ greatly from values measured with the standard method and sometime have no physical meaning.
Non-hygroscopic	Brick, concrete, glass wool, unfired clay	Good prediction. Not necessary to use a hygrothermal model to compare with measurement.

Table 3: Main conclusions of the prediction by the model depending on the type of material

of fibre influences the sorption and the transfer of moisture. Classical models are not relevant to take into account these singularities. Relative humidity kinetics within the material, $\phi_{predicted} = \phi(x_0, t)$, is more difficult to estimate than moisture content, $w_{predicted} = w(t)$ [38]. This highlights a difference in the comparison of a local variable as $\phi(x_0, t)$ and the global value, $w(t)$. The global variable seems to be easier to predict.

For the wall scale, the conclusion depends most on the wall configuration [44]. In buildings, the walls are composed of several layers. Therefore, it is difficult to cross-compare the different cases [20]. Moreover, the results in one layer are influenced by the results and the properties of the other layers [36]. The validation in a multi-layer case, which corresponds to a real case, seems to be the most complex [20]. Concerning the mono-layer walls, the deviations are greater in the centre, as for material scale [44, 43]. For highly hygroscopic materials such as wood or wood fibre, the deviations are substantial with multi-layer walls: the model under-estimates the amplitude and the average value [82] as well as the moisture transport kinetics [90].

The phenomena of heat and moisture transfers are complex to simulate, especially at the material and wall scale when we wish to observe the transport within the material. For these studies, the impact of hygrothermal properties and microscopic structure are greater and may explain the difficulties. For multi-layer walls, the contact between layers also influences the results and increases the problems modelling the heat and mass transfer.

4.2 Boundary conditions

In a building, walls are exposed to variable conditions, and we can therefore assume that the steady-state is never reached within materials. Nevertheless, to validate a model several boundary conditions have to be tested, from easier (controlled and static) to more complex (real and variable). This section compares the modelling performance according to the type of boundary conditions applied to building materials (see Table 4).

For all the studies, the boundary conditions at the air at both sides of the material are expressed by Eq. (4). Some studies considered time-constant conditions, imposing temperature or relative humidity gradients between the two surfaces of the material. In the air at each side of the material the vapour pressure and temperature are expressed:

$$P_{\mathrm{va}} = P^0_{\mathrm{va}}$$
$$T_{\mathrm{a}} = T^0_{\mathrm{a}}$$

with P^0_{va} and T^0_{a}, two constant values for boundary conditions.

In this case, the results appear to be in better agreement in comparison with cyclic conditions [40, 20, 45] where the boundary conditions are time-dependent:

$$P_{\mathrm{va}} = P^0_{\mathrm{va}}(t)$$
$$T_{\mathrm{a}} = T^0_{\mathrm{a}}(t)$$

In this case, the variations are systematically damped by the model and a phase shift appears [82]. The transfer measured seems to be faster than that obtained with simulation. Moreover, the amplitude is greater in the experimental conditions. The conclusions show the same trends for mineral materials as aerated concrete [37] and for bio-based materials [76, 82, 45, 37]. Talukdar et al. [45] also showed that it is easier to model the hygrothermal response of a sample subjected to a relative humidity step than to oscillating conditions.

Non-isothermal boundary conditions also tend to increase the discrepancies between numerical and experimental results, as reported in [76] for wood fibre samples. Similar observations are highlighted in [93]. In the case of real conditions, i.e. when air temperature and relative humidity vary according to outdoor climate, the divergences seem to increase, as reported for wood fibre [76, 27], wood [82, 90] and aerated concrete [37]. The reasons for the discrepancies might be partially explained by the inadequacy of the physical phenomena represented at the bounding surfaces of the material by Eq.(4). Radiation and rain effects, the influence of wind on convective heat transfer coefficients, among others, may be improved in the model.

In the air wind tunnel, an airflow is created on the top of the sample. The experiments were conducted with a relatively low Reynolds number (Re = 1900) to avoid airflow in the material. This is verified in [29]. Moreover, this facility increases the impact of the heat and mass convective transfers by imposing an airflow on the top of the material and could possibly influence the mass transfer within the sample. The measurements are compared with the heat and moisture transfer model without considering air transfer in the material [29, 21, 65]. The agreement is not very good for either, the moisture transfer is faster in reality than in the simulation. We can note that the differences are greater for the cellulose insulation [29], which has a higher air permeability value than the other materials (see Figure 5(a)). Therefore, we can anticipate that modelling the air convection, probably significant in this case with a forced airflow above the material, could improve the agreement between measurement and simulation. Considering the air convection in material could increase the moisture transfer simulated by the numerical tool because the air will transport moisture by advection. Moreover, the numerical results showed that in fibrous insulating material the presence of both diffusion ad convection processes can explain the moisture transfer [106].

When samples are tested under real conditions in field experiments, the prediction of hygrothermal performance seems to be complex for all building materials whatever the model or software used. These difficulties can be related to the model as well as to complex real boundary conditions (radiation, rain, wind), which can also be difficult to measure precisely and to consider in simulation.

4.3 Modelling the physical phenomena

4.3.1 Description and formulation

In this section, bias b_4 (Figure 2), due to the physical model and its mathematical resolution is discussed. As the initial hypothesis, all models consider the same physical phenomena, based on Eq. (1), but they may differ on several points.

First, different physical quantities are used as driving potentials in the mathematical formulation of the equations [107]. Some work has been done with relative humidity [22, 108, 109]. The capillary pressure was used in [87, 110]. The model developed in [111, 112, 113] considers the moisture content as potential and simulations in [28, 27] are carried out with the vapour pressure.

In [114], a model was developed to study the hygrothermal behaviour of *earth-based material*. This model, based on heat and mass balances in the wall, considers the kinematics of each phase separately

Materials	Reference	Boundary conditions	Conclusions
Hemp concrete	[34]	Drying experiment at constant conditions	Faster drying in the experiments (maximum delay: 4 days)
	[35]	Cycle of relative humidity step	Faster variation of temperature and relative humidity in measurements + difference of steady-state value
	[37]	Cyclic conditions	Important underestimation of temperature equilibrium state (1 °C). Different dynamics: slope for relative humidity curve 2.66%RH/h for measurements and 0.4%RH/h for simulation.
Aerated concrete	[37, 88]	Real with constant or cyclic conditions	Water vapour redistribution is much smaller (9%RH) and slower (2 h) than experimental results. Cyclic conditions: daily variations of relative humidity are not represented.
Wood	[82]	Controlled: static and cyclic	Static: Difference of initial slope and equilibrium value (several %RH). Cyclic: Difference of amplitude (more than 4%RH). Variations are damped in the simulation, presence of a phase shift and a difference in average value.
	[90]	Real	Discrepancies lower than 6% of moisture content amplitude. Shape of curve clearly determined with an over-estimation of the average value. Faster sensitivity in reality.
Wood fibre	[76]	Controlled (isothermal, non-isothermal, cyclic)	Isothermal: gap lower than uncertainty for temperature, relative humidity and absolute humidity. Non-isothermal: greater difference for temperature (0.3 °C). For relative humidity and absolute humidity, numerical results are slower at the beginning of the experiment. Dynamic: Temperature error: 0.5 °C. The relative humidity kinetics is damped by simulation + phase shift.
	[27]	Real	Relative humidity daily variation not reproduced + underestimation of global variations (slope: 5.5%RH/day for measurement, 3.75%RH/day for simulation) + 5%RH gap.
Spruce plywood / Cellulose insulation	[45]	Step and cycle	Step: very good agreement for relative humidity (0.35%RH of difference). More deviations for moisture accumulation. Oscillation: more differences (0.7% for relative humidity and 6% for moisture accumulation) + moisture accumulation kinetics is slightly faster than simulation.
Wood frame + mineral wool + OSB	[93]	Real with controlled inside conditions	Constant temperature or daily variation: response well evaluated. Abrupt temperature change: results are slower (slope: for measurement $0.36 g_v/kg_{dryair}/h$ and $0.12 g_v/kg_{dryair}/h$ for simulation) and lower (5% gap for absolute humidity).
Insulation + interior sheathing	[20]	Controlled: constant and cyclic conditions	More sensitive measurements + phase shift for relative humidity. More differences for cyclic conditions (13%RH versus 5%RH).

Table 4: Comparison of results according to the type of boundary conditions for different building materials

(e.g. liquid water, vapour, dry air and solid matrix), in interaction with each other. The impact of some common assumptions in the model was tested:

- Liquid flow is exclusively driven by a relative humidity gradient,
- The variation of vapour mass is negligible.

The results showed that, for rammed earth material, it is necessary to take into account the impact of the thermal gradient on water flow and the variation of vapour mass due to evaporation-condensation. However, the sensitivity analysis done in [114] on the liquid water permeability underlined that these simplifying assumptions can be made for materials with sufficiently low water permeability, which is the case for the most hygroscopic materials.

Some studies showed that it is necessary to consider the heat of sorption in the modelling to predict the hygrothermal behaviour correctly. The difference observed for the temperature could be explained by this phenomenon [78]. The heat of sorption, also named enthalpy of evaporation L_v, can be modelled with some complex equations to take into account the relative humidity dependence with Kelvin's law [114].

Raji [90] showed that it is necessary to consider coupled transfer completely to predict the behaviour of material. Two models were developed to study plain wood walls with in-situ experiments on *CLT* building panels. The first one was a classical model, based on the assumptions of [91]. In the second, energy and mass conservation equations was decoupled. More deviations were observed with the second model (error, 7% in relative humidity versus 3%RH).

Moreover, in modelling the contact between layers is assumed to be perfect but actually this is not the case: taking contact resistance into account can improve modelling results [115].

Diffusion of water vapour can be driven by the vapour pressure gradient or the temperature gradient. The first phenomenon is always considered in the equation while the second one, known as thermal diffusion, is usually ignored. In [107], the author discusses the importance of this assumption, reporting results from other articles. He concludes that in the context of building physics, moisture transport due to the vapour pressure difference is more relevant. Moreover, some studies take into account this effect [33, 39, 27, 72], without reducing the discrepancies in the comparison with experimental data.

As already mentioned, an important hypothesis was postulated on the physical phenomena by not considering air transfer and thus moisture advection in porous materials. In [82], numerical predictions of two different models, `WUFI` [22] and `BuildingPore` [116], were compared. `BuildingPore` considers liquid transport, diffusion and convection of water vapour and the diffusion of adsorbed water. `Wufi` models the transport of the liquid phase and the diffusion of water vapour. Nevertheless, neither one models the air conservation equation. The discrepancies with experimental data are greater for the model that does not consider moisture advection. Similar observations were made in [117], only for moisture advection, considering the experimental data from [21] carried out in the air tunnel facility. The inclusion of an advective term in the model may clearly lead to better results than purely diffusive models. Most particularly, it reduces the gap with the experimental moisture front observed in [21]. Nevertheless, we can question the value of air velocity needed to fit the experimental data.

Other studies point out the importance of air transfer on CLT panels. In [43], `DELPHIN` software was used and the air convection was modelled, whereas in `WUFI` software used in [44], the air conservation equation was not solved. Both studies were based on the same measurements presented in [44]. The results suggest that the difference between measurement and simulation is greater without modelling air transfer (5% moisture content in [44] and 2.7% in [43] at the centre of the panel).

To include heat and moisture advection, the model representing the physical phenomena is improved by including the general equation for dry air mass conservation, also called the continuity equation:

$$\epsilon \, \frac{\partial \rho_{\mathrm{a}}}{\partial t} \;=\; - \boldsymbol{\nabla} \cdot \left(\rho_{\mathrm{a}} \, \mathbf{u} \right), \tag{5}$$

where ϵ is the open porosity of the porous material, ρ_{a} is the dry air density and $\mathbf{u}$ is the velocity. Considering this, two fluxes, depending on the velocity u, are introduced in Eqs. (1b) and (1a), representing heat and moisture advection, respectively:

$$\begin{aligned} \boldsymbol{q}_{\mathrm{a}} &= \rho_{\mathrm{a}} C_p T \mathbf{u}\,, \\ \boldsymbol{g}_{\mathrm{a}} &= \frac{P_{\mathrm{v}}}{R_v T} \mathbf{u}\,. \end{aligned}$$

C_p, R_v refer to the heat capacity of the material and the perfect gas constant for water vapour, respectively.

Moreover, models differ in how they consider the material properties. Most models do not consider the hysteresis effect on moisture storage. Interested readers may refer to [118, 60, 119, 120, 121] for examples taking into account this phenomenon and particularly, in [35], for comparison with experimental data. Let us compare two studies on the same hygroscopic bio-based material, hemp concrete. In [72] the hysteresis effect was not modelled, while in [35] this phenomenon was taken into account, resulting in smaller deviations between numerical and experimental results than in [72] and even lower than experimental uncertainty (bias b_1). Moreover, the temperature dependency of the sorption isotherm was modelled in [51, 74] for hemp concrete and the agreement was better than previous studies [35, 42]. Similar conclusions are observed for another material (spruce) in [62]. The general trend reveals that the models considering the hysteresis effect and the temperature dependency of the moisture storage showed better agreement with experimental data. Nevertheless, considering the hysteresis effect cannot completely explain the difference observed in the moisture transfer kinetics [21, 62].

In [122], the authors doubt the hypothesis of instantaneous hygroscopic equilibrium when a material (wood) is subject to a change in relative humidity. The physical model is improved by integrating a so-called non-Fickian behaviour, represented by a time relaxation in the expression of the boundary condition. The authors only studied this improvement for the moisture conservation equation and the ambient vapour pressure from Eq. (4), written as:

$$P_{\mathrm{va}} = P_{\mathrm{v},\infty} - d \exp\left(\frac{t}{\tau}\right),$$

where τ is the relaxation time and d is a coefficient characterising the amount of bound water molecules. The effect of this modified boundary condition only occurred for the moisture transfer process; the coupling with heat transfer was not taken into account. Nevertheless, the authors concluded that this upgrade fits the numerical model better with the experimental data.

A different non-Fickian model was introduced to model hygrothermal transfer in wood [123, 124]. Such non-Fickian behaviour was highlighted for other fibrous materials: wood fibre [47] and hemp concrete [37]. To take into account this phenomenon, we have to differentiate the adsorption in the fibre and in the pore of the material and the transfer within the material. This is linked to the assumption of local equilibrium, which is challenged for bio-based fibrous materials [76].

Most of the studies considered a one-dimensional transfer through the material. This hypothesis was evaluated in [20] where three models, `1D-HAM`, `MATCH`, and `WUFI-2D`, were compared on full-scale laboratory measurements. The prediction of all three software tools were close for all tests on a wood-frame wall. The study reveals that the one-dimensional hypothesis may be valid for this comparison.

4.3.2 Numerical resolution

In terms of solution computing, most of the numerical approaches consider standard discretisation techniques. Due to its unconditional stability property, the Euler implicit scheme was used in many studies reported in the literature [111, 125, 126, 127, 109, 110, 107, 128]. To increase the level of accuracy in time, the Crank–Nicolson scheme can be used as for instance in [129] . Examples of studies based on an explicit scheme can be found in the literature such as [108, 63, 130]. For spatial discretisation, finite-volume [111, 127, 125] and finite elements [110, 128] are generally adopted. Even

if the studies reported in the literature used different numerical approaches to solve the problem, as soon as the residual of the equation is verified to be less than a fixed tolerance, numerical algorithms may not explain the large discrepancies between the numerical results and the experimental data. Moreover, computer rounding errors can be introduced in the solution, but we believe that they are negligible compared to magnitude of the discrepancies.

4.3.3 Influence of material properties

While reporting previous studies, some deviations between experimental and simulation results, especially for hygroscopic materials, were observed. Some authors concluded saying that the uncertainties of material properties, boundary or initial conditions could explain the deviations. Sensitivity or parametric studies were reported in some of the articles presented above to assess the importance of the model's different input parameters (convective mass transfer coefficient, transport properties, etc.) and their role in the validation process. The main elements and conclusions of these studies are summarised in Table 5.

Different methods can be used to highlight the most influential input parameters. In [28], the reference values were increased one by one by 1% and the output values were observed. Thirteen parameters including the thickness of materials, sorption isotherm and vapour permeability were identified. Then a criterion, based on an uncertainty analysis, made it possible to conclude on the validation of the model. A stochastic approach in which the parameters can take all the values in a probable range is applied in [43]. The method used by the authors, using the partial ranked correlation (PRCC) coefficient, enabled them to conclude on their relative importance and showed that boundary conditions and hygrothermal properties (moisture capacity and vapour permeability) dominated. Nevertheless, the relative role of parameters depends on the wall's configuration (Table 5).

The effect of thermal properties such as dry density, heat capacity and thermal conductivity was studied in [72] for hemp concrete, in [131] for CaSi and in [67] for gypsum. The several percent change applied to each property (10% for [72], 5% for [67]) showed that their impact on temperature and relative humidity results is negligible. The same conclusion was obtained with the sorption heat [29, 64], the convective heat and mass coefficients [45, 131, 64, 21, 131], the air flow rate over the material [131] and specific heat [72].

The impact of the hygrothermal properties is predominant in the hygrothermal behaviour of material and the buffering effect of hygroscopic materials [15]. As mentioned in Section 2, the material vapour permeability is determined using the dry and wet cup methods. However, its ability to characterise all materials adequately was questioned in [132]. The method does not take into account the variation of the total pressure within the cup. Therefore, advective vapour transfer is overlooked. In the case of a highly air-permeable material, this implies that the vapour permeability may be under-estimated. Moreover, the experimental design was carried out in steady-state and isothermal conditions, but in the building physics context, these conditions are never reached.

The sorption isotherm, characterising the moisture capacity of the material, can be changed in the software to determine the value providing the best fit. If the slope of the curve $w = f(\phi)$, usually called $\xi = \frac{\partial w}{\partial \phi}$, characterising the material's ability to store moisture is reduced, the relative humidity variations are greater [131, 64] and the slope of the moisture kinetics increases [45]. Therefore, the sorption capacity of the material predicted by the model using the sorption isotherm curve measured with classical methods is over-estimated. The agreement for moisture and temperature is improved when an intermediate curve between the primary sorption and desorption curves is used [27, 120]. These observations may stem from two other questionable assumptions on the hygrothermal properties. First, the moisture capacity, $\xi = \frac{\partial w}{\partial \phi}$, can have hysteresis between wetting and drying for many materials, as illustrated in Figure 6. Indeed, the behaviour differs between adsorption and desorption processes. Some measurements and effects of hysteresis on the hygric properties are presented in [121] on aerated concrete and cement samples and in [120] on gypsum. The history of the material therefore has an effect on its actual moisture content, which is always between the two primary isotherm curves. Hysteresis is often neglected, however, and only the sorption isotherm is used. Second, the

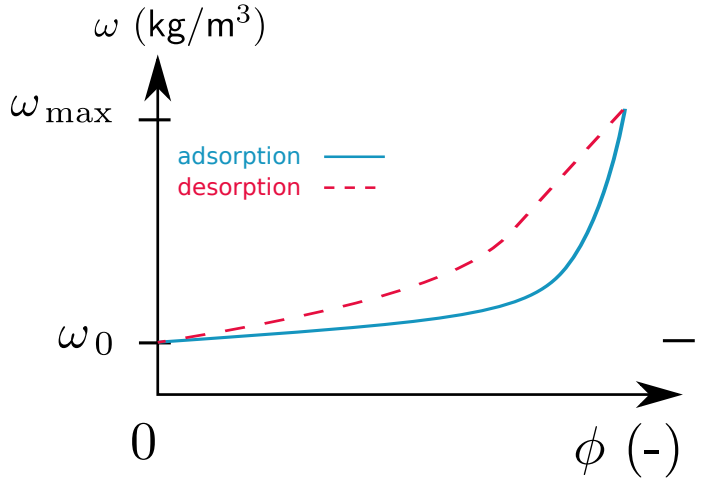

Figure 6: Hysteresis of the sorption curve for adsorption and desorption tests.

sorption curve is often estimated under isothermal conditions. However, some recent studies [62, 50, 61] demonstrated the influence of the temperature on the moisture capacity of the material. Indeed, most of the comparisons made between the numerical results and the experimental data do not take into account these two phenomena.

The other important property is vapour permeability (δ_v) or the vapour resistance factor (μ). The decrease in the vapour resistance factor (μ) leads to greater relative humidity variations [131, 27, 57] and in general also provides better agreement with the experimental results, as it increases the moisture transfer dynamic [38]. Vapour permeability (δ_v) impacts both temperature and relative humidity [45] due to latent heat effects [133].

The best agreement is obtained when both properties (vapour permeability and moisture capacity) are changed simultaneously [42, 133, 21]. The global dynamic is well represented but difficulties remain for the daily fluctuations [27]. The adjusted value of properties can be determined using an inverse method [47, 134, 135, 78]. Published results showed that vapour permeability must nearly be doubled and the slope of sorption isotherm divided by two to obtain the best result with wood fibre material [134, 27].

For the drying experiment [67, 136], the change of the water vapour resistance diffusion factor has no significant impact. Therefore, moisture is presented in the liquid water phase. The change of the water retention curve (adjusted at high capillary pressure) and of liquid permeability (decrease) improves the agreement for moisture distribution and the moisture content curve.

Published articles underlined a mismatch of measured material properties and those which give the best agreement between the numerical models and the experimental results. An increase of the value of the vapour and/or liquid permeability and a decrease of the slope of sorption isotherm and/or retention curve can improve the moisture transport kinetics for several materials (hemp concrete, spruce, wood fibre, calcium silicate, gypsum, cellulose). Nevertheless, no physical meaning was found in these values in terms of giving the best fit.

Reference	Material	Modified parameters	Change	Consequences on results	Conclusions
[42, 35]	Coated hemp concrete	μ, ξ	μ and ξ was decreased	Both parameters: improved prediction of relative humidity variations but not of the mass. Only μ: better prediction of mass variations but not of the relative humidity	Must find compromise to improve both relative humidity and mass variations
[27]	Wood fibre	δ_v, ξ	Doubled vapour permeability; isotherm curve between sorption and desorption	Overall relative humidity dynamics is improved. Daily fluctuations are still not represented	Mismatch of measured material properties and those which give the best agreement.
[28]	Wooden-frame assemblies	Study of 38 parameters	1% increase in each reference value	Thirteen parameters including sorption and permeability are important. Uncertainty analysis ⇒ discrepancies observed during vapour production could be explained by the experimental uncertainties. Validation of the model depends on the position in the wall	Material properties are the most important parameters.
[21]	Gypsum	δ_v, ξ, hysteresis, α, β	10% change in properties	Change of relative humidity level and variations Hysteresis ⇒ agreement in desorption phase but lower influence Slight effect of α and β	Better agreement given by: increase of δ_v + decrease of ξ. Influence of hysteresis and α and β are lower.
[45] [64]	Spruce plywood	ξ, D_m, h_v, λ, α and β	±10% variation in each property	Increase ξ ⇒ lower relative humidity dynamics. D_m ⇒ 2% change in relative humidity and 4% change in temperature. h_v and λ impact temperature only. Results were not directly compared to measurements	Improvement of results: decrease ξ + increase vapour diffusion coefficient
[45] [64]	Cellulose insulation	Same	Same	Sorption curve is more important than others	same
[131]	CaSi	ξ, μ, ρ, β, λ, mass flow rate	Decreased μ and increased ξ	Humidity variations are increased (better agreement). Change of air flow rate, ρ and λ do not affect the results.	Results are improved but amplitude is slightly under-estimated

Reference	Material	Modified parameters	Change	Consequences on results	Conclusions
[70]	CaSi	δ_ℓ, retention curve, μ	μ: 24.79 $\rightarrow$ 32. Retention curve adjusted at high capillary pressure. Decrease of δ_ℓ	μ: no significant impact. Retention curve: improvement for the water content dynamics but not for moisture distribution. δ_ℓ: better overall agreement	Liquid permeability improves drying results
[133]	Gypsum	$\rho, \lambda, C_p, \xi, \delta_\mathrm{v}$	5% change	ρ, C_p and λ: no significant effect. Best agreement with ξ and μ decreased simultaneously, agreement better than 1%.	Impact of hygric properties is greater and provides good agreement between measurement and simulation.
[43]	CLT wall	Environmental conditions, μ, ξ	100 random values in the range of the parameters are tested	Influence on the results quantified with PRCC. Low vapour permeance wall: moisture content level is mainly influenced by the ξ. High vapour permeance wall: the influence of boundary conditions and of ξ is more significant than μ.	Influencing parameters depend on the assembly configuration.
[15]	Gypsum / wood	Comparison of two materials with different properties	Wood vs. gypsum: higher ξ and μ	Residual moisture for wood $\Rightarrow$ great importance of moisture history. Lower adsorption during short cycle for wood, similar to gypsum for a longer load cycle. Lower penetration depth for wood.	Great impact of the value of δ_v and ξ on the hygrothermal behaviour.
[72]	Hemp concrete	ξ, δ_v, C_p, ρ, λ, α and β	10% variation	Hygric physical properties are the most influential parameters.	Comparison between measurement and simulation is not improved.

Table 5: Summary of sensitivity studies

5 Conclusion

The impact of the coupled heat and mass transfers on buildings must be taken into account to have a better understanding of the building's performance [90, 82, 3, 137, 11, 4]. The models are used to predict the transfers within walls. To validate the representation of physical phenomena using the model, the comparison with experimental measurement is necessary.

This study showed that the agreement between the experimental measurement and the numerical results have to be improved at both the material and wall scales. These observations hold true especially for moisture fields: moisture content, relative humidity and vapour pressure. Nevertheless, the global fields (average moisture content) show slightly smaller deviations between measurement and simulation than the local variables (relative humidity for example). The results show that it is more difficult to predict the transfer kinetics than the values in steady-state. Therefore, deviations appear when the samples are subjected to fast dynamic solicitations such as temperature steps[93, 138], relative humidity steps [38, 131, 67], cyclic conditions [82, 20, 36, 45, 15, 42] and real conditions [88, 28, 43]. The errors are greater with highly hygroscopic and bio-based materials, wood-based materials, cellulose and hemp concrete, than for traditional construction materials such as concrete or brick. On the other hand, the temperature is relatively accurately predicted by the models, the deviations are most often within the experimental uncertainties. Nevertheless, the deviations could be caused by modelling of the heat of sorption.

The materials' properties play a crucial role for the agreement of results. The general trend reveals that the model considering the hysteresis effect [35, 42] and temperature dependency of the moisture storage [51], showed better agreement with experimental data. However, the prediction of moisture transfer kinetics is not always improved when considering the hysteresis effect [62]. Several studies highlight that the vapour permeability or the diffusivity used in the codes is lower than the real effect observed in the materials, because the measured relative humidity variations vary faster than predicted [82]. The moisture content and relative humidity curve are also influenced by the change of the sorption isotherm curve slope. These results seem to prove that the hygrothermal properties measured on the materials with standard methods in steady-state (cup method, gravimetric) does not accurately reproduce the hygrothermal transfers under dynamic load, which is the case for the building envelope. New dynamic experimental methods are currently being developed [47, 38]. The transport properties determined using the inverse method [134, 57, 139, 135, 78, 102] confirm this, because the values giving the best agreement between measurements and simulations are completely different from the measured values. Given this substantial difference, the values of adapted properties tend to show that the model is not complete for highly hygroscopic materials. Some phenomena seem not to be considered (advection of air, non-equilibrium state and microscopic effects). This could explain the differences observed between measurement and simulation and could add physical meaning to the adapted properties. To improve model prediction it is necessary to question the model's assumptions, such as the modelling of air transfer [117] or the local-equilibrium hypothesis with microscopic effects [47, 37, 140].

Acknowledgments

This work was funded by French Environment and Energy Management Agency (ADEME), through CAPVENT project, "Assemblée des pays de Savoie" (APS), and the French National Research Agency (ANR) through its Sustainable Cities and Buildings program (MOBAIR project n°ANR-12-VBDU-0009).

References

[1] J. Berger, S. Guernouti, M. Woloszyn, C. Buhe, Factors governing the development of moisture disorders for integration into building performance simulation, Journal of Building Engineering 3 (2015) 1 – 15. doi:http://dx.doi.org/10.1016/j.jobe.2015.04.008.

[2] N. Mendes, F. Winkelmann, R. Lamberts, P. Philippi, Moisture effects on conduction loads, Energy and Buildings 35 (7) (2003) 631–644.

[3] F. Antretter, C. Mitterer, S.-M. Young, Use of moisture-buffering tiles for indoor climate stability under different climatic requirements, HVAC&R Research 18 (1-2) (2012) 275–282.

[4] M. Liu, Y. Zhu, B. Park, D. E. Claridge, D. K. Feary, Airflow reduction to improve building comfort and reduce building energy consumption–a case study, ASHRAE Transactions 105 (1999) 384.

[5] H. Viitanen, J. Vinha, K. Salminen, T. Ojanen, R. Peuhkuri, L. Paajanen, K. Lahdesmaki, Moisture and Bio-deterioration Risk of Building Materials and Structures, Journal of Building Physics 33 (3) (2010) 201–224. doi:10.1177/1744259109343511.

[6] M. Salonvaara, T. Ojanen, A. H. Holm, H. M. Künzel, A. Karagiozis, Moisture buffering effects on indoor air quality-experimental and simulation results, Proceedings of Buildings IX (2004) 11.

[7] L. Fang, G. Clausen, P. O. Fanger, Impact of temperature and humidity on the perception of indoor air quality, Indoor air 8 (2) (1998) 80–90.

[8] C. Simonson, M. Salonvaara, T. Ojanen, The effect of structures on indoor humidity–possibility to improve comfort and perceived air quality, Indoor Air 12 (4) (2002) 243–251.

[9] M. Woloszyn, T. Kalamees, M. O. Abadie, M. Steeman, A. S. Kalagasidis, The effect of combining a relative-humidity-sensitive ventilation system with the moisture-buffering capacity of materials on indoor climate and energy efficiency of buildings, Building and Environment 44 (3) (2009) 515–524.

[10] S. Hameury, Influence of coating system on the moisture buffering capacity of panels of pinus sylvestris l., Wood Material Science and Engineering 2 (3-4) (2007) 97–105.

[11] O. F. Osanyintola, C. J. Simonson, Moisture buffering capacity of hygroscopic building materials: experimental facilities and energy impact, Energy and Buildings 38 (10) (2006) 1270–1282.

[12] H. Yoshino, T. Mitamura, K. Hasegawa, Moisture buffering and effect of ventilation rate and volume rate of hygrothermal materials in a single room under steady state exterior conditions, Building and Environment 44 (7) (2009) 1418–1425. doi:10.1016/j.buildenv.2008.09.007.

[13] M. Woloszyn, T. Kalamees, M. Olivier Abadie, M. Steeman, A. Sasic Kalagasidis, The effect of combining a relative-humidity-sensitive ventilation system with the moisture-buffering capacity of materials on indoor climate and energy efficiency of buildings, Building and Environment 44 (3) (2009) 515–524. doi:10.1016/j.buildenv.2008.04.017.

[14] X. Yang, H. Ge, P. Fazio, J. Rao, Evaluation of Parameters Influencing the Moisture Buffering Potential of Hygroscopic Materials with BSim Simulations, Buildings 4 (3) (2014) 375–393. doi:10.3390/buildings4030375.

[15] H. Ge, X. Yang, P. Fazio, J. Rao, Influence of moisture load profiles on moisture buffering potential and moisture residuals of three groups of hygroscopic materials, Building and Environment 81 (2014) 162–171. doi:10.1016/j.buildenv.2014.06.021.

[16] Künzel, H.M., Sedlbauer, K, Holm, A, Antretter, F., Ellinger, M, Moisture buffering effects of interior linings made from wood or wood based products (2004).

[17] Y. Li, P. Fazio, J. Rao, An investigation of moisture buffering performance of wood paneling at room level and its buffering effect on a test room, Building and Environment 47 (2012) 205–216. doi:10.1016/j.buildenv.2011.07.021.

[18] M. Woloszyn, C. Rode, Tools for performance simulation of heat, air and moisture conditions of whole buildings, Building Simulation (2008) 5–24.

[19] J. Delgado, N. M. Ramos, E. Barreira, V. De Freitas, A critical review of hygrothermal models used in porous building materials, Journal of Porous Media 13 (3).

[20] T. Kalamees, J. Vinha, Hygrothermal calculations and laboratory tests on timber-framed wall structures, Building and Environment 38 (5) (2003) 689–697. doi:10.1016/S0360-1323(02)00207-X.

[21] C. James, C. J. Simonson, P. Talukdar, S. Roels, Numerical and experimental data set for benchmarking hygroscopic buffering models, International Journal of Heat and Mass Transfer 53 (19-20) (2010) 3638–3654. doi:10.1016/j.ijheatmasstransfer.2010.03.039.

[22] H. M. Künzel, Simultaneous heat and moisture transport in building components.

[23] C. Hagentoft, A. S. Kalagasidis, A. Adl-Zarrabi, Assessment method of numerical prediction models for combined heat, air and moisture transfer in building components. benchmarks for one-dimensional cases, Journal of thermal envelope and building science (27) (2004) 327–352.

[24] H. Janssen, B. Blocken, J. Carmeliet, Conservative modelling of the moisture and heat transfer in building components under atmospheric excitation, International Journal of Heat and Mass Transfer 50 (5–6) (2007) 1128 – 1140. doi:http://dx.doi.org/10.1016/j.ijheatmasstransfer.2006.06.048.

[25] H. Cagnon, J. Aubert, M. Coutand, C. Magniont, Hygrothermal properties of earth bricks, Energy and Buildings 80 (2014) 208–217. doi:10.1016/j.enbuild.2014.05.024.
URL http://linkinghub.elsevier.com/retrieve/pii/S0378778814004162

[26] Hygrothermal performance of building materials and products — determination of water vapour transmission properties, ISO NF 12572.

[27] Y.-A. Kedowide, Analyses expérimentales et numériques du comportement hygrothermique d'une paroi composée de matériaux fortement hygroscopiques, Ph.D. thesis, Grenoble Alpes (2015).

[28] M. Labat, M. Woloszyn, G. Garnier, J. J. Roux, Dynamic coupling between vapour and heat transfer in wall assemblies: Analysis of measurements achieved under real climate, Building and Environment 87 (2015) 129–141. doi:10.1016/j.buildenv.2015.01.022.

[29] P. Talukdar, S. O. Olutmayin, O. F. Osanyintola, C. J. Simonson, An experimental data set for benchmarking 1-D, transient heat and moisture transfer models of hygroscopic building materials. Part I: Experimental facility and material property data, International Journal of Heat and Mass Transfer 50 (23–24) (2007) 4527 – 4539. doi:http://dx.doi.org/10.1016/j.ijheatmasstransfer.2007.03.026.

[30] O. F. Osanyintola, C. J. Simonson, Effect of initial conditions, boundary conditions and thickness on the moisture buffering capacity of spruce plywood, Energy and Buildings 38 (10) (2006) 1283–1292. doi:10.1016/j.enbuild.2006.03.023.

[31] N. Zogzas, Z. Maroulis, D. Marinos-Kouris, Moisture deffusivity methods of experimental determination areview, Drying technology 12 (3) (1994) 483–515.

[32] E. Agoua, S. Zohoun, P. Perré, A double climatic chamber used to measure the diffusion coefficient of water in wood in unsteady-state conditions: determination of the best fitting method by numerical simulation, International journal of heat and mass transfer 44 (19) (2001) 3731–3744.

[33] M. Qin, A. Aït-Mokhtar, R. Belarbi, Two-dimensional hygrothermal transfer in porous building materials, Applied Thermal Engineering 30 (16) (2010) 2555–2562. doi:10.1016/j.applthermaleng.2010.07.006.

[34] A. Evrard, A. De Herde, Hygrothermal Performance of Lime-Hemp Wall Assemblies, Journal of Building Physics 34 (1) (2010) 5–25. doi:10.1177/1744259109355730.

[35] D. Lelievre, T. , P. Glouannec, Hygrothermal behavior of bio-based building materials including hysteresis effects: Experimental and numerical analyses, Energy and Buildings 84 (2014) 617–627. doi:10.1016/j.enbuild.2014.09.013.

[36] J. Carmeliet, D. Derome, Temperature driven inward vapor diffusion under constant and cyclic loading in small-scale wall assemblies: Part 1 experimental investigation, Building and Environment 48 (2012) 48–56. doi:10.1016/j.buildenv.2011.08.015.

[37] D. Samri, Analyse physique et caractérisation hygrothermique des matériaux de construction: approche expérimentale et modélisation numérique, Ph.D. thesis, INSA Lyon (2008).

[38] T. Busser, A. Piot, M. Pailha, T. Bejat, M. Woloszyn, From materials properties to modelling hygrothermal transfers of highly hygroscopic walls, in: CESBP, Dresden, Germany, 2016.

[39] R. Belarbi, M. Qin, A. Aït-Mokhtar, L.-O. Nilsson, Experimental and theoretical investigation of non-isothermal transfer in hygroscopic building materials, Building and Environment 43 (12) (2008) 2154–2162. doi:10.1016/j.buildenv.2007.12.014.

[40] J. Carmeliet, D. Derome, Temperature driven inward vapor diffusion under constant and cyclic loading in small-scale wall assemblies: Part 2 heat-moisture transport simulations, Building and Environment 47 (2012) 161–169. doi:10.1016/j.buildenv.2011.07.028.

[41] J. del Coz Díaz, F. Álvarez Rabanal, O. Gencel, P. García Nieto, M. Alonso-Martínez, A. Navarro-Manso, B. Prendes-Gero, Hygrothermal study of lightweight concrete hollow bricks: A new proposed experimental–numerical method, Energy and Buildings 70 (2014) 194–206. doi:10.1016/j.enbuild.2013.11.060.

[42] T. Colinart, D. Lelievre, P. Glouannec, Experimental and numerical analysis of the transient hygrothermal behavior of multilayered hemp concrete wall, Energy and Buildings 112 (2016) 1–11. doi:10.1016/j.enbuild.2015.11.027.

[43] L. Wang, H. Ge, Hygrothermal performance of cross-laminated timber wall assemblies: A stochastic approach, Building and Environment 97 (2016) 11–25. doi:10.1016/j.buildenv.2015.11.034.

[44] R. McClung, H. Ge, J. Straube, J. Wang, Hygrothermal performance of cross-laminated timber wall assemblies with built-in moisture: field measurements and simulations, Building and Environment 71 (2014) 95–110. doi:10.1016/j.buildenv.2013.09.008.

[45] P. Talukdar, O. F. Osanyintola, S. O. Olutimayin, C. J. Simonson, An experimental data set for benchmarking 1-D, transient heat and moisture transfer models of hygroscopic building materials. Part II: Experimental, numerical and analytical data, International Journal of Heat and Mass Transfer 50 (25–26) (2007) 4915 – 4926. doi:http://dx.doi.org/10.1016/j.ijheatmasstransfer.2007.03.025.

[46] Z. Zhang, M. Thiery, V. Baroghel-Bouny, Numerical modelling of moisture transfers with hysteresis within cementitious materials: Verification and investigation of the effects of repeated wetting–drying boundary conditions, Cement and Concrete Research 68 (2015) 10–23. doi:10.1016/j.cemconres.2014.10.012.

[47] P. Perré, F. Pierre, J. Casalinho, M. Ayouz, Determination of the Mass Diffusion Coefficient Based on the Relative Humidity Measured at the Back Face of the Sample During Unsteady Regimes, Drying Technology 33 (9) (2015) 1068–1075. doi:10.1080/07373937.2014.982253.

[48] M. Van Belleghem, M. Steeman, A. Willockx, A. Janssens, M. De Paepe, Benchmark experiments for moisture transfer modelling in air and porous materials, Building and Environment 46 (4) (2011) 884–898. doi:10.1016/j.buildenv.2010.10.018.

[49] S. Dubois, A. Evrard, F. Lebeau, Modeling the hygrothermal behavior of biobased construction materials, Journal of Building Physics 38 (3) (2014) 191–213. doi:10.1177/1744259113489810.

[50] X. Zhang, W. Zillig, H. M. Künzel, C. Mitterer, X. Zhang, Combined effects of sorption hysteresis and its temperature dependency on wood materials and building enclosures-part II: Hygrothermal modeling, Building and Environment 106 (2016) 181–195. doi:10.1016/j.buildenv.2016.06.033.

[51] Colinart, T, Glouannec, P, ACCOUNTING FOR THE TEMPERATURE DEPENDENCE IN THE SORPTION ISOTHERMS IN THE PREDICTION OF HYGROTHERMAL BEHAVIOR OF HEMP CONCRETE, Dresde, 2016.

[52] Y. Mualem, A modified dependent-domain theory of hysteresis., Soil Science 137 (5) (1984) 283–291.

[53] J. Rubin, Numerical method for analyzing hysteresis-affected, post-infiltration redistribution of soil moisture, Soil Science Society of America Journal 31 (1) (1967) 13–20.

[54] A. Evrard, Transient hygrothermal behaviour of lime-hemp materials, PhD, Université Catholique De Louvain.

[55] P. Perré, I. W. Turner, A 3-d version of transpore: a comprehensive heat and mass transfer computational model for simulating the drying of porous media, International Journal of heat and mass transfer 42 (24) (1999) 4501–4521.

[56] M. Woloszyn, J. Virgone, Hygro-bat : Vers une méthode de conception hygro-thermique des batiments performants. rapport final.

[57] S. Rouchier, T. Busser, M. Pailha, A. Piot, M. Woloszyn, Hygric characterization of wood fiber insulation under uncertainty with dynamic measurements and markov chain monte-carlo algorithm, Building and Environment 114 (2017) 129–139.

[58] S. Roels, J. Carmeliet, H. Hens, Hamstad wp1: Final report - moisture transfer properties and materials characterization.

[59] S. Roels, J. Carmeliet, H. Hens, O. Adan, H. Brocken, R. Cerny, Z. Pavlik, C. Hall, K. Kumaran, L. Pel, et al., Interlaboratory comparison of hygric properties of porous building materials, Journal of thermal envelope and building science 27 (4) (2004) 307–325.

[60] P. F., C. Rode, Prediction of moisture transfer in building constructions, Building and Environment 27 (3) (1992) 387–397. doi:10.1016/0360-1323(92)90038-Q.

[61] T. Colinart, P. Glouannec, Temperature dependence of sorption isotherm of hygroscopic building materials. part 1: Experimental evidence and modeling, Energy and Buildings 139 (2017) 360–370.

[62] X. Zhang, W. Zillig, H. M. Künzel, C. Mitterer, X. Zhang, Combined effects of sorption hysteresis and its temperature dependency on wood materials and building enclosures – Part I: Measurements for model validation, Building and Environment 106 (2016) 143–154. doi:10.1016/j.buildenv.2016.06.025.

[63] A. S. Kalagasidis, P. Weitzmann, T. Nielsen, R. Peuhkuri, C.-E. Hagentoft, C. Rode, The international building physics toolbox in simulink, Energy and Buildings 39 (6) (2007) 665–674. doi:10.1016/j.enbuild.2006.10.007.

[64] S. O. Olutimayin, C. J. Simonson, Measuring and modeling vapor boundary layer growth during transient diffusion heat and moisture transfer in cellulose insulation, International Journal of Heat and Mass Transfer 48 (16) (2005) 3319–3330. doi:10.1016/j.ijheatmasstransfer.2005.02.024.

[65] H. J. Steeman, M. Van Belleghem, A. Janssens, M. De Paepe, Coupled simulation of heat and moisture transport in air and porous materials for the assessment of moisture related damage, Building and Environment 44 (10) (2009) 2176–2184. doi:10.1016/j.buildenv.2009.03.016.

[66] Fluent.

[67] M. Van Belleghem, M. Steeman, A. Janssens, M. De Paepe, Drying behaviour of calcium silicate, Construction and Building Materials 65 (2014) 507–517. doi:10.1016/j.conbuildmat.2014.04.129.

[68] T. Defraeye, Convective Heat and Mass Transfer at Exterior Building Surfaces, Ph.D. thesis (2011).

[69] H. Derluyn, H. Janssen, J. Carmeliet, Influence of the nature of interfaces on the capillary transport in layered materials, Construction and Building Materials 25 (9) (2011) 3685–3693.

[70] M. Van Belleghem, M. Steeman, H. Janssen, A. Janssens, M. De Paepe, Validation of a coupled heat, vapour and liquid moisture transport model for porous materials implemented in CFD, Building and Environment 81 (2014) 340–353. doi:10.1016/j.buildenv.2014.06.024.

[71] N. Mendes, I. Ridley, R. Lamberts, P. C. Philippi, K. Budag, UMIDUS: a PC program for the prediction of heat and moisture transfer in porous building elements, in: Building Simulation Conference–IBPSA, Vol. 99, 1999, pp. 277–283.

[72] C. Maalouf, A. T. Le, S. Umurigirwa, M. Lachi, O. Douzane, Study of hygrothermal behaviour of a hemp concrete building envelope under summer conditions in France, Energy and Buildings 77 (2014) 48–57. doi:10.1016/j.enbuild.2014.03.040.

[73] T. Colinart, P. Glouannec, T. Pierre, P. Chauvelon, A. Magueresse, Experimental study on the hygrothermal behavior of a coated sprayed hemp concrete wall, Buildings 3 (1) (2013) 79–99.

[74] A. Le, D. Samri, M. Rahim, O. Douzane, G. Promis, C. Maalouf, M. Lachi, T. Langlet, Effect of temperature-dependent sorption characteristics on the hygrothermal behavior of a hemp concrete building envelope submitted to real outdoor conditions, Journal of Applied Fluid Mechanics 9 (2016) 245–252.

[75] A. FABBRI, P.-A. CHABRIAC, D. T. NGO, F. SALLET, E. GOURDON, H. Wong, J.-C. Morel, Hygrothermal behaviour of hemp concrete; experimental evidences and modelling, 2015.

[76] SLIMANI, Zakaria, Analyse expérimentale et numérique du comportement hygrothermique de parois fortement hygroscopiques, Ph.D. thesis, CETHIL, Université de Lyon (2015).

[77] F. Tariku, K. Kumaran, P. Fazio, Transient model for coupled heat, air and moisture transfer through multilayered porous media, International Journal of Heat and Mass Transfer 53 (15-16) (2010) 3035–3044. doi:10.1016/j.ijheatmasstransfer.2010.03.024.

[78] D. Medjelekh, L. Ulmet, F. Gouny, F. Fouchal, B. Nait-Ali, P. Maillard, F. Dubois, Characterization of the coupled hygrothermal behavior of unfired clay masonries: Numerical and experimental aspects, Building and Environment 110 (2016) 89–103.

[79] CEA, Cast3m, finite element software, www.cast3M.cea.fr.

[80] S. Merakeb, F. Dubois, C. Petit, Modeling of the sorption hysteresis for wood, Wood science and technology 43 (7-8) (2009) 575.

[81] H. Rafidiarison, R. Rémond, E. Mougel, Dataset for validating 1-D heat and mass transfer models within building walls with hygroscopic materials, Building and Environment 89 (2015) 356–368. doi:10.1016/j.buildenv.2015.03.008.

[82] H. Rafidiarison, Etudes expérimentales des transferts de masse et de chaleur dans les parois des constructions en bois, en vue de leur modélisation. Applications aux économies d'énergie et au confort dans l'habitat, Ph.D. thesis, Ecole Nationale Supérieure des Technologies et Industries du Bois (2012).

[83] B. T. Hagentoft C-E., 1d-ham coupled heat, air and moisture transport in multi-layered wall structures. manual with brief theory and an example, Version 2.0.

[84] C. Rode, Combined heat and moisture transfer in building construction, Ph.D. thesis (1990).

[85] J. Vinha, Hygrothermal performance of timber-framed external walls in Finnish climatic conditions: a method for determining the sufficient water vapour resistance of the interior lining of a wall assembly, Ph.D. thesis, Tampere (2007).

[86] X. Yang, P. Fazio, H. Ge, J. Rao, Evaluation of moisture buffering capacity of interior surface materials and furniture in a full-scale experimental investigation, Building and Environment 47 (2012) 188 – 196, international Workshop on Ventilation, Comfort, and Health in Transport Vehicles. doi:http://dx.doi.org/10.1016/j.buildenv.2011.07.025.

[87] Q. Li, J. Rao, P. Fazio, Development of HAM tool for building envelope analysis, Building and Environment 44 (5) (2009) 1065–1073. doi:10.1016/j.buildenv.2008.07.017.

[88] F. Tariku, M. K. Kumaran, Hygrothermal modeling of aerated concrete wall and comparison with field experiment, in: Proceeding of the 3rd International Building Physics/Engineering Conference, 2006, pp. 26–31.

[89] M. Salonvaara, A. Karagiozis, Moisture transport in building envelopes using an approximate factorization solution method, in: CFD Society of Canada, 1994, 1994.

[90] S. Raji, Caractérisation hygro-thermique, par une approche multi échelle, de constructions en bois massif en vue d'amélioration énergétique et de valorisation environnementale, Ph.D. thesis, thèse de doctorat dirigée par Puiggali, Jean-Rodolphe et Lagière, Philippe Sciences physiques et de l'ingénieur. Sciences du bois Bordeaux 1 2006 2006BOR13335 (2006).

[91] J. Philip, D. De Vries, Moisture movement in porous materials under temperature gradients, Eos, Transactions American Geophysical Union 38 (2) (1957) 222–232.

[92] A. Piot, M. Woloszyn, J. Brau, C. Abelé, Experimental wooden frame house for the validation of whole building heat and moisture transfer numerical models, Energy and Buildings 43 (6) (2011) 1322–1328. doi:10.1016/j.enbuild.2011.01.008.

[93] A. Piot, Hygrothermique du bâtiment : expérimentation sur une maison à ossature bois en conditions climatiques naturelles et modélisation numérique, Ph.D. thesis, Institut National des Sciences Appliquées (INSA) de Lyon (2009).

[94] M. Labat, Chaleur – Humidité – Air dans les maisons à ossature bois : Expérimentation et modélisation, Ph.D. thesis, thèse de doctorat dirigée par Roux, Jean-Jacques et Woloszyn, Monika Génie civil Lyon, INSA 2012 2012ISAL0115 (2012).

[95] M. Ibrahim, E. Wurtz, P. H. Biwole, P. Achard, H. Sallee, Hygrothermal performance of exterior walls covered with aerogel-based insulating rendering, Energy and Buildings 84 (2014) 241–251. doi:10.1016/j.enbuild.2014.07.039.

[96] R. Galliano, K. G. Wakili, T. Stahl, B. Binder, B. Daniotti, Performance evaluation of aerogel-based and perlite-based prototyped insulations for internal thermal retrofitting: Hmt model validation by monitoring at demo scale, Energy and Buildings 126 (2016) 275–286.

[97] A. Teasdale-St-Hilaire, D. Derome, Comparison of experimental and numerical results of wood-frame wall assemblies wetted by simulated wind-driven rain infiltration, Energy and Buildings 39 (11) (2007) 1131–1139. doi:10.1016/j.enbuild.2006.12.004.

[98] M. Abuku, B. Blocken, S. Roels, Moisture response of building facades to wind-driven rain: field measurements compared with numerical simulations, Journal of Wind Engineering and Industrial Aerodynamics 97 (5) (2009) 197–207.

[99] W. Maref, M. A. Lacasse, D. Booth, others, Benchmarking of IRC's Advanced Hygrothermal Model–hygIRC Using Mid-and Large-scale Experiments, Tech. rep., NRC, Institute for Research in Construction (2002).

[100] W. Maref, D. G. Booth, M. Lacasse, M. Nicholls, Drying Experiment of Wood-Frame Wall Assemblies Performed in the Climatic Chamber EEEF.

[101] W. Maref, K. Kumaran, M. Lacasse, M. Swinton, D. Van Reenen, Laboratory measurements and benchmarking of an advanced hygrothermal model, HEAT TRANSFER 3 (2002) 117–122.

[102] J. Berger, T. Busser, D. Dutykh, N. Mendes, On the estimation of moisture permeability and advection coefficients of a wood fibre material using the optimal experiment design approach, submitted.

[103] C. Rode, K. Grau, Integrated calculation of hygrothermal conditions of buildings, in: Proceedings of the 6th Symposium on Building Physics in the Nordic Countries, Vol. 1, Norwegian University of Science and Technology, 2002, pp. 23–30.

[104] R. American Society of Heating, A. C. Engineering, ASHRAE Handbook—Fundamentals, Chapter 26: Heat, Air, and Moisture Control in Building Assemblies—Material Properties, 2013.

[105] M. Kumaran, Iea annex 24 final report, vol. 3, task 3: Material properties, IEA, Acco Leuven, Leuven.

[106] K. Abahri, R. Bennacer, R. Belarbi, Sensitivity analyses of convective and diffusive driving potentials on combined heat air and mass transfer in hygroscopic materials, Numerical Heat Transfer, Part A: Applications 69 (10) (2016) 1079–1091. doi:10.1080/10407782.2015.1109389. URL http://www.tandfonline.com/doi/full/10.1080/10407782.2015.1109389

[107] H. Janssen, Simulation efficiency and accuracy of different moisture transfer potentials, Journal of Building Performance Simulation 7 (5) (2014) 379–389. doi:10.1080/19401493.2013.852246.

[108] F. Tariku, K. Kumaran, P. Fazio, Transient model for coupled heat, air and moisture transfer through multilayered porous media, International Journal of Heat and Mass Transfer 53 (15–16) (2010) 3035–3044. doi:10.1016/j.ijheatmasstransfer.2010.03.024.

[109] H.-J. Steeman, M. Van Belleghem, A. Janssens, M. De Paepe, Coupled simulation of heat and moisture transport in air and porous materials for the assessment of moisture related damage, Building and Environment 44 (10) (2009) 2176–2184. doi:10.1016/j.buildenv.2009.03.016.

[110] S. Rouchier, M. Woloszyn, G. Foray, J. Roux, Influence of concrete fracture on the rain infiltration and thermal performance of building facades, International Journal of Heat and Mass Transfer 61 (2013) 340–352. doi:10.1016/j.ijheatmasstransfer.2013.02.013.

[111] N. Mendes, P. C. Philippi, A method for predicting heat and moisture transfer through multilayered walls based on temperature and moisture content gradients, International Journal of Heat and Mass Transfer 48 (1) (2005) 37–51. doi:10.1016/j.ijheatmasstransfer.2004.08.011.

[112] R. M. Barbosa, N. Mendes, Combined simulation of central {HVAC} systems with a whole-building hygrothermal model, Energy and Buildings 40 (3) (2008) 276 – 288. doi:http://dx.doi.org/10.1016/j.enbuild.2007.02.022.

[113] G. H. D. Santos, N. Mendes, Combined heat, air and moisture (ham) transfer model for porous building materials, Journal of Building Physics 32 (3) (2009) 203–220. doi:10.1177/1744259108098340.

[114] L. Soudani, A. Fabbri, J.-C. Morel, M. Woloszyn, P.-A. Chabriac, H. Wong, A.-C. Grillet, Assessment of the validity of some common assumptions in hygrothermal modeling of earth based materials, Energy and Buildings 116 (2016) 498–511.

[115] J. Langmans, R. Klein, S. Roels, Numerical and experimental investigation of the hygrothermal response of timber frame walls with an exterior air barrier, Journal of Building Physics 36 (4) (2013) 375–397. doi:10.1177/1744259112473934.

[116] R. Rémond, P. Perré, Modélisation du Comportement Thermique d'une Maison Bois à l'Aide de Micromodèles Chaleur-Masse Distribués, International Building Performance Simulation Association (IBPSA)-France.

[117] J. Berger, S. Gasparin, D. Dutykh, N. Mendes, How to accurately predict moisture front?, submitted.

[118] Y. Aït Oumériane, M. Bart, S. Moissette, C. Lanos, S. Prétot, F. Collet, Hygrothermal behaviour of a hemp concrete wall: influence of sorption modelling, in: 9th Nordic Symposium on building Physics, Finland, 2011.

[119] J. Carmeliet, M. De Wit, H. Janssen, Hysteresis and moisture buffering of wood, in: Symposium of Building Physics in the Nordic Countries, Citeseer, 2005, pp. 55–62.

[120] J. Kwiatkowski, M. Woloszyn, J.-J. Roux, Modelling of hysteresis influence on mass transfer in building materials, Building and Environment 44 (3) (2009) 633–642. doi:10.1016/j.buildenv.2008.05.006.

[121] P. Crausse, J. Laurent, B. Perrin, Influence des phénomènes d'hystérésis sur les propriétés hydriques de matériaux poreux: Comparaison de deux modèles de simulation du comportement thermohydrique de parois de bâtiment, Revue générale de Thermique 35 (410) (1996) 95–106.

[122] W. Olek, R. Rémond, J. Weres, P. Perré, Non-fickian moisture diffusion in thermally modified beech wood analyzed by the inverse method, International Journal of Thermal Sciences 109 (2016) 291 – 298. doi:http://dx.doi.org/10.1016/j.ijthermalsci.2016.06.023.

[123] L. Wadsö, Describing non-Fickian water-vapour sorption in wood, Journal of Materials Science 29 (9) (1994) 2367–2372.

[124] H. L. Frandsen, L. Damkilde, S. Svensson, A revised multi-fickian moisture transport model to describe non-fickian effects in wood, Holzforschung 61 (5) (2007) 563–572.

[125] F. IBP, Wufi, http://www.hoki.ibp.fhg.de/wufi/wufi_frame_e.html.

[126] Pontifical Catholic University of Parana PUCPR, Domus, http://www.domus.pucpr.br/.

[127] B. Bauklimatik Dresden, Simulation program for the calculation of coupled heat, moisture, air, pollutant, and salt transport, http://www.bauklimatik-dresden.de/delphin/index.php?aLa=en.

[128] H. Janssen, B. Blocken, J. Carmeliet, Conservative modelling of the moisture and heat transfer in building components under atmospheric excitation, International Journal of Heat and Mass Transfer 50 (5–6) (2007) 1128–1140. doi:10.1016/j.ijheatmasstransfer.2006.06.048.

[129] M. van Genuchten, A comparison of numerical solutions of the one-dimensional unsaturated—saturated flow and mass transport equations, Advances in Water Resources 5 (1) (1982) 47 – 55. doi:http://dx.doi.org/10.1016/0309-1708(82)90028-8.

[130] S. Gasparin, J. Berger, D. Dutykh, N. Mendes, Numerical schemes for the solution of nonlinear moisture transfer in porous materials: implicit or explicit? that is the question!, CoRR abs/1701.07059.
URL http://arxiv.org/abs/1701.07059

[131] M. Steeman, M. Van Belleghem, M. De Paepe, A. Janssens, Experimental validation and sensitivity analysis of a coupled BES–HAM model, Building and Environment 45 (10) (2010) 2202–2217. doi:10.1016/j.buildenv.2010.04.003.

[132] T. Duforestel, Des transferts couplés de masse et de chaleur à la conception bioclimatique: recherches sur l'efficacité énergétique des bâtiments., HDR, Université d'Artois.

[133] M. Van Belleghem, H.-J. Steeman, M. Steeman, A. Janssens, M. De Paepe, Sensitivity analysis of CFD coupled non-isothermal heat and moisture modelling, Building and Environment 45 (11) (2010) 2485–2496. doi:10.1016/j.buildenv.2010.05.011.

[134] S. Rouchier, M. Woloszyn, Y. Kedowide, T. Béjat, Identification of the hygrothermal properties of a building envelope material by the covariance matrix adaptation evolution strategy, Journal of Building Performance Simulation (ahead-of-print) (2015) 1–14.

[135] S. Dubois, F. McGregor, A. Evrard, A. Heath, F. Lebeau, An inverse modelling approach to estimate the hygric parameters of clay-based masonry during a moisture buffer value test, Building and Environment 81 (2014) 192–203. doi:10.1016/j.buildenv.2014.06.018.

[136] T. Defraeye, B. Blocken, J. Carmeliet, Influence of uncertainty in heat–moisture transport properties on convective drying of porous materials by numerical modelling, Chemical Engineering Research and Design 91 (1) (2013) 36–42.

[137] M. Qin, G. Walton, R. Belarbi, F. Allard, Simulation of whole building coupled hygrothermal-airflow transfer in different climates, Energy Conversion and Management 52 (2) (2011) 1470–1478. doi:10.1016/j.enconman.2010.10.010.

[138] S. Dubois, F. Lebeau, Impact des matériaux biosourcés sur le climat intérieur: Un outil de calcul flexible à l'échelle de la pièce, Paris, 2014.

[139] J. Berger, H. R. Orlande, N. Mendes, S. Guernouti, Bayesian inference for estimating thermal properties of a historic building wall, Building and Environment 106 (2016) 327–339.

[140] H. Künzel, A. Holm, D. Zirkelbach, A. Karagiozis, Simulation of indoor temperature and humidity conditions including hygrothermal interactions with the building envelope, Solar Energy 78 (4) (2005) 554–561. doi:10.1016/j.solener.2004.03.002.

Nomenclature

A: exposed surface of the sample (m^2)
c_ℓ: heat capacity at constant pressure of liquid water ($\mathsf{J/(Kg\,K)}$)
C_p: heat capacity at constant pressure of material ($\mathsf{J/(Kg\,K)}$)
d: coefficient characterizing the amount of bound water molecules
D_m: vapour diffusion coefficient
Δx: thickness of sample (m)
E: internal energy ($\mathsf{J/m^3}$)
f: moisture diffusivity ($\mathsf{m^2/s}$)
$\boldsymbol{g}$: mass flux ($\mathsf{kg/(s\,m^2)}$)
h_v: water vapour sorption enthalpy ($\mathsf{J/(kg)}$
h_l: liquid water mass sorption enthalpy ($\mathsf{J/kg}$)
L_v: latent heat evaporation of water ($\mathsf{J/kg}$)
m: mass (kg)
P: pressure (Pa)
Pc: capillary pressure (Pa)
Pv: vapour pressure (Pa)
$\boldsymbol{q}$: heat flux ($\mathsf{W/m^2}$)
$\boldsymbol{q}_{\mathrm{c}}$: heat flux by conduction ($\mathsf{W/m^2}$)
R_v: perfect gas constant of water vapour ($\mathsf{J/(Kg\,K)}$)
t: time (s)
T: temperature (K)
u: velocity ($\mathsf{m/s}$)
w: moisture content ($\mathsf{kg_{water}/m^3}$)
x: coordinate in the sample of material (m)

Greek symbols

α: convective heat transfer coefficient ($\mathsf{W/(m^2\,K)}$)
β: convective mass transfer coefficient ($\mathsf{m/s}$)
δ: permeability ($\mathsf{kg/(m\,s\,Pa)}$)
δ_{T}: permeability for temperature driven vapour diffusion ($\mathsf{kg/(m\,s\,K)}$)
$\delta_{v,a}$: water vapour permeability of air ($\mathsf{kg/(m\,s\,Pa)}$)
ϵ: porosity (-)
ξ: moisture capacity = slope of sorption isotherm curve ($\mathsf{kg/m^3}$)
λ: thermal conductivity ($\mathsf{W/(K\,m)}$)
μ: diffusion resistance factor
ϕ: air relative humidity
ρ: density ($\mathsf{kg/m^3}$)
τ: relaxation time (s)

Subcripts
a: air
c: conduction
∞: boundary conditions in surrounding air
l: liquid water
lv: vaporisation
observed: observed value
predicted: predicted value
v: water vapour

Abreviations
CaSi: Calcium Silicate
CFD: Computational Fluid Dynamic
CLT: Cross Laminated Timber
HAM: Heat, Air and Moisture
HC: hemp concrete
MBV: Moisture Buffering Value
OSB: Oriented Strand Board
PRCC: Partial Ranked Correlation Coefficient
TMT: Transient Moisture Transfer